Acadia University Institute

Report # 34
March 1987

Prepared under contract for Supply and Services Canada, Contract Serial No. ST85-00429, DSS File No. 41ST.23216-5-7326

DEVELOPMENT OF HYDRODYNAMIC MODEL IN CUMBERLAND BASIN FOR TIDAL POWER APPLICATIONS

(UP-A-444)

FINAL REPORT
MARCH 1987

Sylvain de Margerie [1]

Dave DeWolfe [2]

[1] ASA Consulting Ltd.
P.O. Box 2025, Dartmouth East
Dartmouth, Nova Scotia, B2W 3X8

[2] Discovery Consultants Ltd.
P.O. Box 599
Wolfville, Nova Scotia, B0P 1X0

EXECUTIVE SUMMARY

Cumberland Basin has recently been identified as a likely candidate for tidal power development. The large scale effect of harnessing tidal power in the Bay of Fundy and the Gulf of Maine has already been investigated but the implications on the local hydrodynamic regime of Cumberland Basin had remained largely unexplored. A substantial effort in the advancement of our knowledge of the hydrodynamics of this area is described in this report. It describes the use of a fine-grid, three dimensional hydrodynamic model which is used to describe the tidal and current patterns in Cumberland Basin for both the natural regime and a regime modified by the installation of a tidal power barrage (A8) between Peck's Point and Boss Point.

The model was used to assess the impact of the A8 tidal power project on the tidal regime of Cumberland Basin. The A8 barrage, location, and operating characteristics were incorporated into the model, and used to calculate the barrage-induced modifications to both the tidal regime and the residual circulation patterns, for both the conventional arrangement of the proposed A8 barrage as well as the A8 barrage altered by re-arranging the location of the sluices and turbines.

This model reproduces the vertical and horizontal flow characteristics of Cumberland Basin with the highest resolution presently practical with large main frame computers (the longest runs requiring up to 240 hours of CPU time on a CDC CYBER 830). This model and the associated data base should provide the best basis for impact studies of tidal power development on the ecosystem, sediment and morphological regimes of Cumberland Basin, as well as to study the effects on turbidity distribution and benthic and pelagic organisms.

As part of this study, a 28 day high quality record of water levels was collected in Cumberland Basin. This, together with a data set collected independently by Mount Allison University, was analyzed to provide the best estimates of tidal parameters for Cumberland Basin. All available bathymetric soundings for the area were evaluated and corrected for changes in datum and horizontal references through time, to form a new consolidated bathymetric data set. These tidal and bathymetric data are available in digital form and are a valuable output of the study.

An examination of available data, as well as a theoretical analysis, has shown that tidal flows dominate the hydrodynamic regime of Cumberland Basin. Tidal flows exhibit a marked vertical structure, both in the oscillatory and mean components, which can only be fully accounted for by a three-dimensional analysis. To this end, an advanced mathematical model was constructed for Cumberland Basin, modified to account for mudflats and salt marshes which dry for part of the tidal cycle and represent about half of the area of Cumberland Basin. In this model, the vertical flow structure is represented continuously by a set of basis functions, a method producing more realistic profiles than discrete techniques and generally considered a preferred tool for 3-D modelling. This three dimensional representation reproduces explicitly the phenomena of vertical shear dispersion and topographically induced eddies which drive dispersion and transport mechanisms in Cumberland Basin.

A sensitivity analysis, as well as consideration of the basin topography, has confirmed that the most important length scales of Cumberland Basin are resolved by a grid size of 400m in the horizontal, and the use of six basis functions for the representation of the vertical profile. The model shows only moderate sensitivity to the specification of bottom drag coefficient and vertical turbulent diffusivity profile. Notably, the bottom stress computed from the model is much less sensitive

to the specification of drag coefficient than 2-D models, reflecting the equilibrium relationship between the flow structure and bottom boundary conditions. This should provide more reliable estimates of bottom stress for applications such as sediment transport.

The model has been verified for forcing by the single M_2 tidal frequency, as well as a full fortnightly tidal cycle with all major tidal constituents. Model calculations agree with observations within measurement accuracy. Simulations were also undertaken with the presence of a tidal barrage between Pecks Point and Boss Point (site A8). The main simulation, using a likely configuration for the placement of sluices and turbines, shows that, as expected, the tidal range, currents and bottom stresses in the head pond will be drastically reduced from natural conditions. A second simulation was undertaken with sluices and turbines placed at opposite ends of the barrages in shallower portions of the basin. The effects on tidal range were similar to the first configuration, but a large amount of variability and eddy motion was generated in the head pond. This may be attributed to the increased water velocities which at times approaches the shallow water wave celerity and, in combination with bottom topography, may induce flow instabilities.

The data sets generated in this study include simulated water levels and velocity coefficients (characterizing the vertical flow structure) for each model cell, at 15 minute time intervals, for a 14 day period (a tidal fortnight). The same is also available for 4 day simulations using M_2 tidal forcing alone, with and without the presence of a barrage. Although many analyses may be undertaken, depending on the application, only the most basic processing has been undertaken here. Further work on these data sets will depend on the specific application, but the following are of a general interest:

- Analysis of post barrage stratification potential using the H/U^3 method (Garrett et al, 1978).

- Computation of effective flushing times, horizontal and vertical mixing rates, etc.

- Computation of turbulent energy distribution.

- Calculation of the 3-D residual and tidal flow patterns through selected cross-sections.

The model software can also be used to generate new data sets, for example, to investigate the effect of alternate barrage geometries. Further hydrodynamic modelling studies should be undertaken to consider the effects of wind and waves, which may have a significant effect on the mean circulation of the basin, as well as on the bottom stress distribution.

ACKNOWLEDGMENTS

We are grateful to Tony Tung, the Scientific Authority, and the Unsolicited Proposals Program of the Department of Supply and Services, for helping to bring this work to fruition. We would also like to thank Dave Greenberg of the Bedford Institute of Oceanography and George Baker of the Nova Scotia Tidal Power Corporation for their valuable and willing assistance and advice. Thanks are due to Alan Mac Ewan and the Computer Center Staff at Acadia University for providing extra support to the project when it was needed. Karen Lank, Steve Hurlbut, Steve Marquis, and Susan Davidson of ASA Consulting Ltd., all helped in bringing this work to completion. Paul Cant, of the Physics Department, Mount Allison University, provided helpful comments about Cumberland Basin and furnished the Fort Beausejour bottom pressure data.

STUDY PARTICIPANTS

Acadia University Institute

Dr. Marshall W. Conley, Executive Director
Dr. Maurice Tugwell, Acting Executive Director
Dr. Graham R. Daborn, Scientific Advisor
Miss Darlene M. Feener, Secretary

ASA Consulting Ltd.

Mr. Stephen E. Hurlbut, Modeller
Mr. Sylvain de Margerie, Modeller
Mr. Steven Marquis, Programmer
Ms. Karen Lank, Programmer

Applied Sciences Associates Inc.

Dr. Malcolm L. Spaulding, Advisor
Mr. Tatsusaburo Isaji, Advisor

Discovery Consultants Ltd.

Mr. David L. DeWolfe, Project Co-ordinator and Modeller

TABLE OF CONTENTS

PAGE

EXECUTIVE SUMMARY i
ACKNOWLEDGMENTS v
TABLE OF CONTENTS vi
LIST OF TABLES vii
LIST OF FIGURES viii

1.0 INTRODUCTION 1
1.1 Background 1
Bay of Fundy Tides 2
Description of Cumberland Basin 2
1.2 Review of Previous Work 3
1.3 Study Objectives 8

2.0 TIDAL MEASUREMENTS AND ANALYSIS 9
2.1 Introduction and Objectives 9
2.2 The Historical Tidal Data 11
2.3 The Field Program 13
Additional Data 14
2.4 Data Analysis and Results 15

3.0 DEVELOPMENT OF THE HYDRODYNAMIC MODEL 20
3.1 Introduction and Objectives 20
3.2 General Hydrodynamic Considerations 21
3.3 Mathematical Model Description 26
3.4 Bathymetry 34
Model Bathymetry 37
3.5 Boundary Conditions 38
Open Boundaries 38
Coastal Boundaries 40
3.6 Calibration 40
3.7 Verification 41
3.8 Sensitivity Analysis 44
3.9 Simulation of the Fortnightly Tidal Cycle 49

4.0 MODEL APPLICATIONS 55
4.1 Introduction 55
4.2 The A8 Barrage 55
4.3 The Pre-Barrage Tidal Regime 58
4.4 Barrage Operational Scenarios 58
4.5 The Post-Barrage Tidal Regime 60
4.6 High Current Locations for Current Driven Turbines 72

5.0 CONCLUSIONS AND RECOMMENDATIONS 73

6.0 BIBLIOGRAPHY 78

APPENDIX A Model Set-up 82

APPENDIX B Barrage Set up 88

APPENDIX C Model Output and Analysis of Results 91

APPENDIX D Glossary of Oceanographic and Technical Terms .. 95

APPENDIX E Photographs 98

LIST OF TABLES

PAGE

Table 2-1 Summary of tidal observations taken in the Cumberland Basin area. 12

Table 2-2 Amplitude and phase lag of the tidal constituents calculated from the bottom pressure record observed in May - June, 1986. 18

Table 2-3 Amplitude and phase lag of the tidal constituents calculated from the bottom pressure record observed in August and September 1983, by Mt. Allison University. 19

Table 3-1 Amplitude and phase of the principal tidal constituents at the seaward boundary of the model. 38

Table 3-2 Agreement between model and observations for M_2 tidal elevations. 43

Table 3-3 Sensitivity analysis from M_2 simulation. 51

Table 4-1 Coefficients of the least squares fitted equations used to simulate the flow for the A8 turbine. 56

Table 4-2 Comparison of the pre- and post-barrage tidal elevations in Cumberland Basin. 60

Table 4-3 Comparison of mean head pond level and tidal amplitude 61

LIST OF FIGURES

		PAGE
Figure 1-1	Current sampling stations in Cumberland Basin	6
Figure 1-2	Vertical structure of the flow and suspended sediment concentration	7
Figure 2-1	Cumberland Basin study area	10
Figure 2-2	Plot of the 1986 tidal data recorded near Wood Point	16
Figure 2-3	Periodograms of the Fort Beausejour (1983) and Wood Point(1986) tidal data	17
Figure 3-1	Legendre polynomial representation of the vertical structure.	31
Figure 3-2	Coarse grid model and model variable definition	32
Figure 3-3	Fine grid model and bathymetry	39
Figure 3-4	M_2 cotidal chart for natural conditions	42
Figure 3-5	Comparison of model results with observations at Minudie Wharf	45
Figure 3-6	Sensitivity of the vertical velocity profile at ebb tide.	48
Figure 3-7	Tidal range computed from a fortnightly simulation	52
Figure 3-8	Mean bottom stress (scalar) from a fortnightly simulation	53
Figure 3-9	Depth mean residual currents from a fortnightly simulation	54
Figure 4-1	Flow characteristics of a single turbine at A8.	57

Figure 4-2	Mean magnitude of bottom stress (scalar) for the M_2 tide, under natural conditions	59
Figure 4-3	M_2 current regime at flood tide, under natural conditions	63
Figure 4-4	M_2 current regime at ebb tide, under natural conditions.	64
Figure 4-5	M_2 current regime at low tide, under natural conditions.	65
Figure 4-6	Current regime in Cumberland Basin with the A8 barrage in operation, at low tide.	66
Figure 4-7	Current regime in Cumberland Basin with the A8 barrage in operation, at high tide.	67
Figure 4-8	Difference in mean magnitude of bottom stress due to barrage operation	68
Figure 4-9	Tidal currents at low tide with a modified barrage configuration.	70

1.0 INTRODUCTION

1.1 Background

The Bay of Fundy has been the focus of study for potential tidal power development since 1919. Engineering surveys were conducted in 1945 (Acres, 1946), 1969 (ATPPB, Atlantic Tidal Power Programming Board), and 1977 (TPRB, Tidal Power Review Board) to verify this potential. The TPRB (1977) study demonstrated the engineering and economic feasibility of tidal power for selected sites in Minas and Cumberland Basins. The tidal power schemes suggested subsequently for these sites are single basin, single effect types where power generation takes place only for 5-6 hours during the ebb portion of the tidal cycle. Refilling of the basin would then occur during the flooding tide. The tidal range in the head pond region for a barrage near the mouth of the basin (see Figure 2-1) would be reduced by about 50% with both local increases and decreases in current speed. The overall impact suggested by Greenberg's (1979) hydrodynamic model studies is a reduction in local tidal energy available for sediment transport but with a corresponding increase in energy in the Gulf of Maine.

Although considerable amounts of data have been collected in the Cumberland Basin, no detailed analysis has been undertaken to investigate the effect of a barrage near the mouth of the basin (site A8), the most likely candidate for first construction.

Bay of Fundy Tides

The Bay of Fundy/Gulf of Maine tidal system has a natural period of approximately 13 hours (Garrett, 1972) and is in near resonance with the semi-diurnal tides of the North Atlantic. The M_2 tide is amplified from a 1 metre range at the edge of the continental shelf to somewhat over 12 metres in the upper portion of Minas Basin. Only the semi-diurnal components of the tide are amplified; the other components of the tide do not vary appreciably throughout the system. In Cumberland Basin, the maximum tidal range is about 14.6 metres, and the mean tidal range about 11 metres.

Description of Cumberland Basin

Cumberland Basin is situated at the head of the Bay of Fundy and is bounded by the shores of both Nova Scotia and New Brunswick. It covers a total area of about 100 km^2, of which about 40% are mudflats and 17% saltmarsh which are dry at low tide. The hydrodynamic regime of Cumberland Basin is entirely dominated by tides, with elevations and currents at least an order of magnitude greater than even the most extreme disturbances due to wind stress or other effects. The quantity of water in Cumberland Basin varies dramatically over the course of a tidal cycle, the volume varying from about 1.3 km^3 at high tide to 0.03

km^3 at low tide. At low water, the bottom of the Basin upstream of Fort Beausejour is essentially a stream carrying the runoff of the tidal channels and rivers that flow into the basin. The level of suspended sediment in the basin is extremely high, reaching as much as 1000 mg/l, or more.

1.2 Review of Previous Work.

The consideration of the tidal power generation as well as scientific curiosity has prompted many studies of the Bay of Fundy. The general hydrodynamic character of the Bay has been investigated by Godin (1968), Garrett (1972, 1974, 1977), Greenberg (1969, 1975, 1983) and Rao (1968) to name only a few. These studies explain the high tidal amplitude in this area by the near resonant response of the Bay at the predominant semidiurnal tidal frequency. Investigations of the effect of energy exploitation at several promising sites show that one can expect changes in tidal amplitude throughout the Bay of Fundy and the Gulf of Maine (Greenberg, 1979; Garrett, 1974) and that the headpond waters could become stratified (Garrett, Keeley and Greenberg, 1978). Most detailed analyses have however been centered on Minas Basin where observations were used to calibrate fine grid mathematical models, which suggest that both the residual currents (Tee, 1977) and sedimentation (Greenberg and Amos, 1982) would not be drastically altered by the presence of a barrage at the mouth of Cobequid Bay.

To date no detailed hydrodynamic study of Cumberland Basin has been undertaken, although a substantial amount of effort has been put in the analysis of its ecosystem (Gordon etal, 1986). Greenberg has included Cumberland Basin in his numerical studies, however the coarse resolution of his model (only 22 cells representing the Basin) provides only a first cut at the problem. Holloway (1981) has considered Cumberland Basin in his analysis of mixing in the bay of Fundy, but again puts most of his attention on Minas Basin. Amos and Asprey (1981) give a description of tidal flows in Chignecto Bay and Cumberland Basin based on observations, however their interest lies principally in the sediment transport patterns for the area. The data on which their study is based are well described in Hildebrand et al, (1980) and represent most of the site specific information available for Cumberland Basin. Relevant stations from this study are shown in Figure 1-1 and consist primarily of two current meter moorings location and of a series of profiling stations each occupied for a tidal cycle near the mouth of the Basin. Not shown is a network of bottom sampling stations. These data show that tidal current amplitudes generally range between 1 m/s and 2 m/s. Figure 1-2, extracted from Amos and Asprey (1981), shows the marked vertical structure of the flow and suspended sediment concentration at certain stages of the tide. Although the sediment concentrations shown in this plot are higher than usual (100 mg/l to 400 mg/l), it shows that, at times, suspended material concentrations are sufficient to cause substantial density differences, which may

influence the flow. Also evident from this data is the asymmetry between the ebb and flood tides. Averaging these velocities over a tidal cycle one can see that the mean residual flow also exhibits vertical shear, with outflowing currents dominating near the surface.

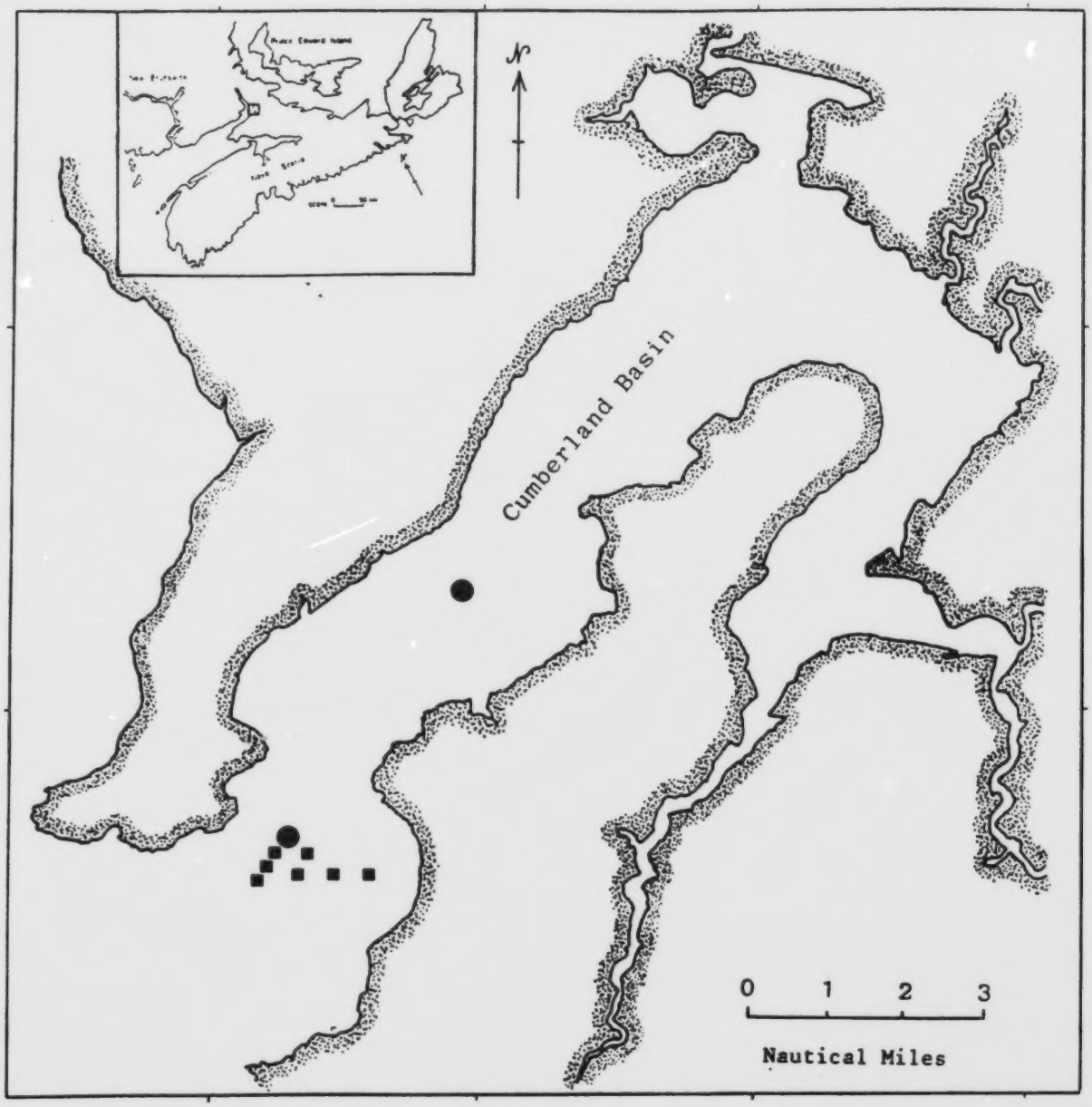

● Moored Current Meter Station

■ Hand Held Current Meter Station

Figure 1-1 Current sampling stations in Cumberland Basin

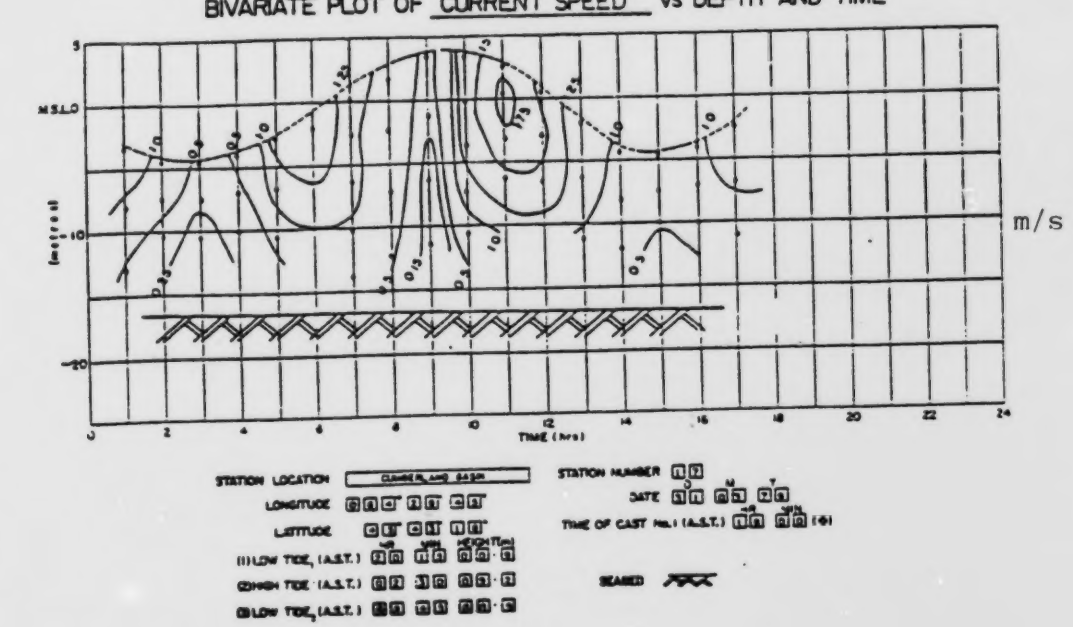

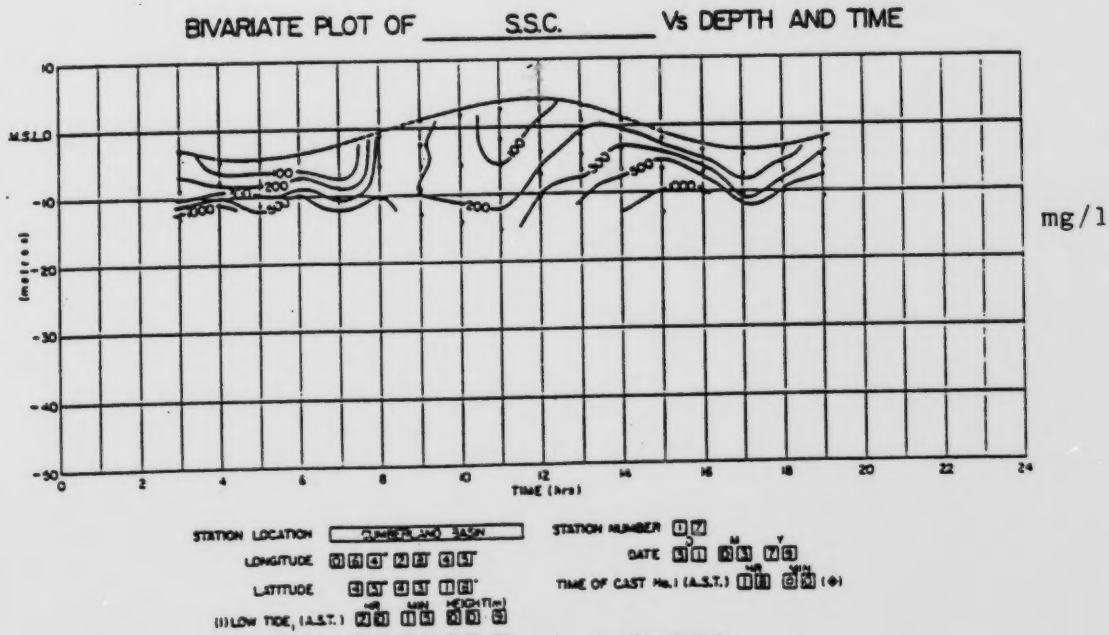

Figure 1-2 Vertical structure of the flow and suspended sediment concentration (from Amos and Asprey, 1981)

1.3 Study Objectives

There are two principal objectives of this work:

1. to develop a high resolution hydrodynamic model capable of describing the principal hydrodynamic processes affecting Cumberland Basin

2. to examine the tidal barrage-induced modification to the tidal regime of Cumberland Basin and the circulation patterns under various possible operational scenarios, and to determine possible limits of tidal plant operational strategies in order to minimize the regime changes.

An additional objective of this work is to identify and recommend possible high tidal current locations in the Cumberland Basin, for the purpose of making future assessments of the feasibility of small scale tidal power applications, based on kinetic energy extraction from the flow.

The development of a coarse (800 m) grid model and then a fine (400 m) model is discussed in Sections 2 and 3, and the applications of the model are discussed in Section 4.2.

2.0 TASK 1 - TIDAL MEASUREMENT AND ANALYSIS

2.1 Introduction and Objectives

Few tidal observations have been made in Cumberland Basin. At the commencement of this project, tidal sea elevations at the open boundary (seaward side) of the Cumberland Basin werewell described by the modelling results of Greenberg (1979) as well as by observations, but there was a lack of high quality tidal observations further up the estuary past Peck's Point.

To ensure rigorous calibration of the models in this area, an accurate set of observations of the vertical tide at an interior location in the Cumberland Basin was obtained.

The objective of the task 1 program was to obtain an accurate set of tidal measurements toverifyand calibrate the hydrodynamic model at an interior point about mid-way up the basin. This particular area (see Fig. 2-1) was as far as possible from the mouth of the basin, yet in deep enough water to ensure with some margin of safety that the gauge would remain submerged at low tide. It was chosen to portray the modification of the tidal signal as it propagates up the basin.

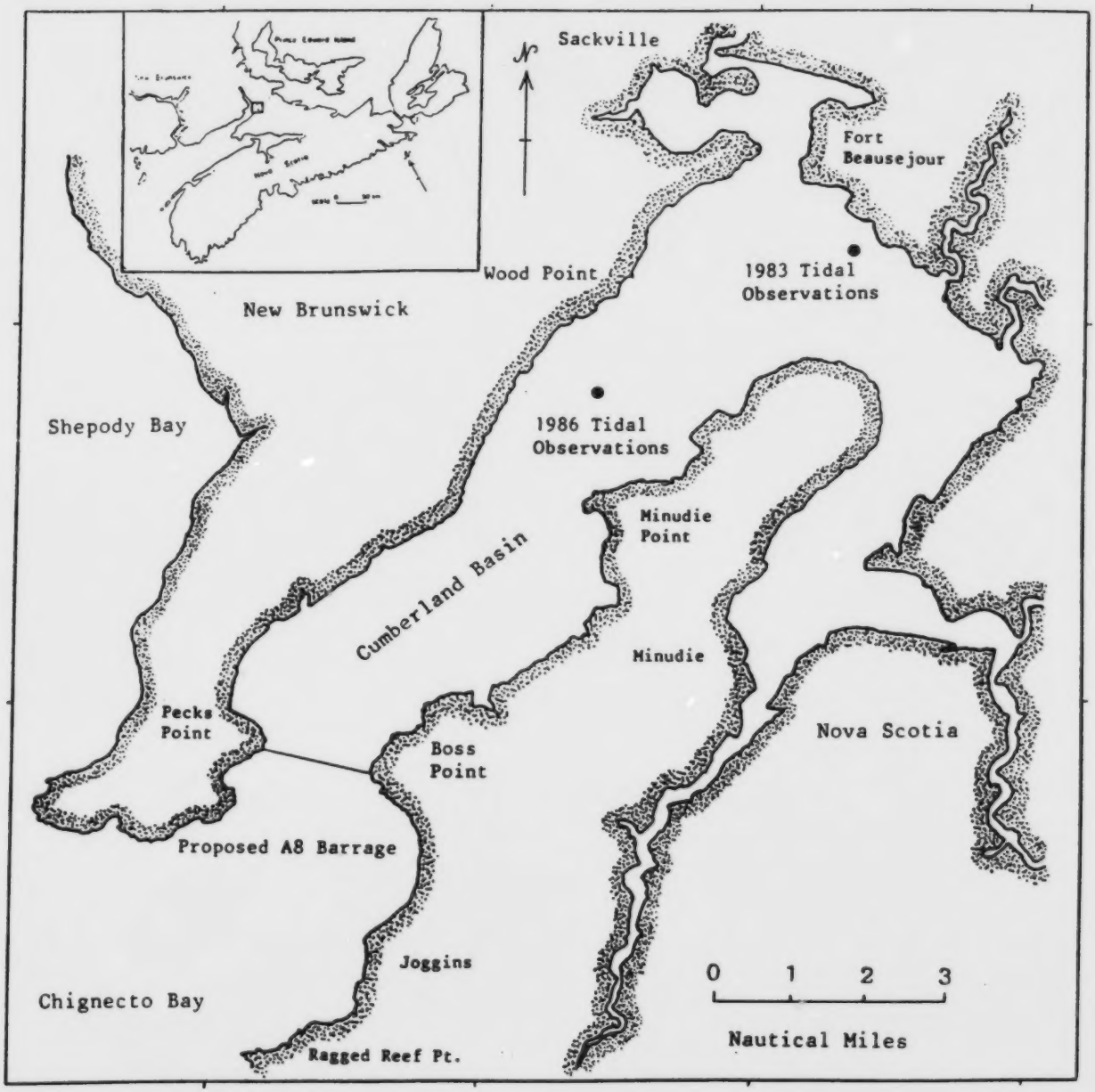

Figure 2.1 Cumberland Basin study area.

With any program of oceanographic observations carried out in a dynamic marine environment such as Cumberland Basin, there exists a certain element of risk with respect to the recovery of moored instrumentation. In Cumberland Basin, the overall risk is increased because of the greatly reduced visibility due to the high suspended sediment load, and the strong currents. The mooring package was an instrument platform (see photograph, Appendix E) firmly placed on the bottom and secured in both the upstream and downstream directions by about 35 metres of groundline, each stretching to an anchor. Likelihood of recovery of the package was enhanced by the use of three separate pingers; two on the instrument platform and one at the end of one of the groundlines. The acoustic signals emitted by the pingers would enable a diver to home in on the gear, irrespective of the visibility.

2.2 The Historical Tidal Data

Tidal measurements were first made in the Cumberland Basin area in the mid-1800's as part of the British Admiralty hydrographic charting program. These observations were relatively short and somewhat lacking in precision. Since the late 1960's, there has been an increase in interest in the Cumberland Basin resulting from the tidal power studies. The first high quality tidal observations were made in 1976. A summary of the observations in the Cumberland Basin area up to and including this present work is presented in Table 2-1.

Prior to the 1976 work (DeWolfe, 1977), tidal observations were undertaken with a shore based gauge and a long capillary tube extending across the intertidal zone to a pressure sensor on the bottom. These devices are subject to error when used with long capillary tubes and for large tidal ranges. The data obtained subsequently with direct measuring seabed recorders are of much better quality than those previously obtained.

Table 2-1 Summary of tidal observations in and around Cumberland Basin.

Date	Area	Lat.	Long.	Duration
1986	Wood Point	45-49.4 N	64-22.8 W	28 days
1983	Fort Beausejour	45-50.9 N	64-17.9 W	30 days
1976	Ragged Reef	45-40 N	64-31 W	77 days
1976	Grindstone	45-43 N	64-36 W	87 days
1965	Pecks Point	45-45 N	64-29 W	29 days
1919	Joggins Wharf	45-41 N	64-28 W	29 days

The Admiralty tidal data is obscure and is not included.

2.3 The Field Program

The field program was divided into two portions. The purpose of the first part was to deploy the tide gauge for a period of about one month in the area indicated on Figure 2-1. An additional objective was to obtain soundings on drying flats which were previously uncharted. The necessary oceanographic equipment (an Aanderaa WLR-5 bottom pressure recorder, three Helle Pingers and a pinger locator device) was leased from Seastar Instruments Ltd. in Dartmouth and the mooring hardware and miscellaneous equipment was procured locally. A 13 m fishing vessel based in Cumberland Basin was chartered. The second part of the field program was to return about one month later, recover the equipment and obtain more soundings if necessary.

The first phase of the field program took place on 29 April 1986 with the mooring being deployed at 1500 hrs AST without difficulty. After deployment, some bathymetric data were collected over the large mudflat south of Minudie Point.

Phase 2 of the field program was carried out on 27 May 1986. A first attempt to recover the tide gauge mooring was undertaken at the morning low tide. The vessel was however unable to lift the mooring without the aid of a diver and due to the extremely short period of slack water, the recovery was delayed until the afternoon high tide. More soundings were taken on the mudflat

south of Minudie Point while waiting for the high tide. Prior to high tide, the site of the mooring was again occupied. The instrument package was recovered and brought aboard at 1500 AST. All gear was in working order. A plot of the data is shown in Figure 2-2.

Additional Data

A tidal record taken by the Physics Dept. at Mt. Allison University was made available to the project (Cant 1986). This one month bottom pressure record was taken in August and September 1983 in the location shown in Figure 2-1. As a tidal harmonic analysis had not been performed on these data at Mt. Allison, the data were obtained and analyzed as part of this project. A cubic spline was fitted to these data (sampled at an interval of 10.733 minutes), and the hourly values calculated. The data were then analyzed by standard methods (Foreman, 1977). The results are shown in Table 2-3. Comparison of the harmonic analyses for the 1986 data at Wood Point and the 1983 data at Fort Beausejour shows a number of interesting features which are attributable to differences in location. For example, the Fort Beausejour data (1983) shows that the semi-diurnal tidal components are smaller than at Wood Point (1986) which is located closer to the mouth of the basin. On the other hand, high frequency components are more predominant in the Fort Beausejour data. These differences are characteristic of the propagation of large amplitude waves in

shallow water and are due to friction and nonlinear transformation of the wave.

2.4 Data Analysis and Results

The raw data were decoded to obtain hourly pressures and analyzed using conventional techniques (Foreman, 1977) to estimate the amplitude and phase of all important tidal constituents (Tables 2-2 and 2-3). It should be noted that the large amplitudes for some of the fourth and sixth diurnals are a result of the non-linear distortions of the tidal signal by the so called shallow water effects. The time of arrival of the high tide is 5 minutes later at Fort Beausejour than it is at Wood Point, but the time of arrival of low tide at Fort Beausejour is 23 minutes later, due to the distortion of the tidal wave.

Shallow water effects in the upper reaches of Cumberland Basin are evident in the spectra of Figure 2-3. At the location of the 1986 tidal data, only the second and third harmonics of the semi-diurnal (M_4 and M_6) signal have significant amplitude. By the time the signal reaches Fort Beausejour the higher harmonic content extends to the fifth harmonic.

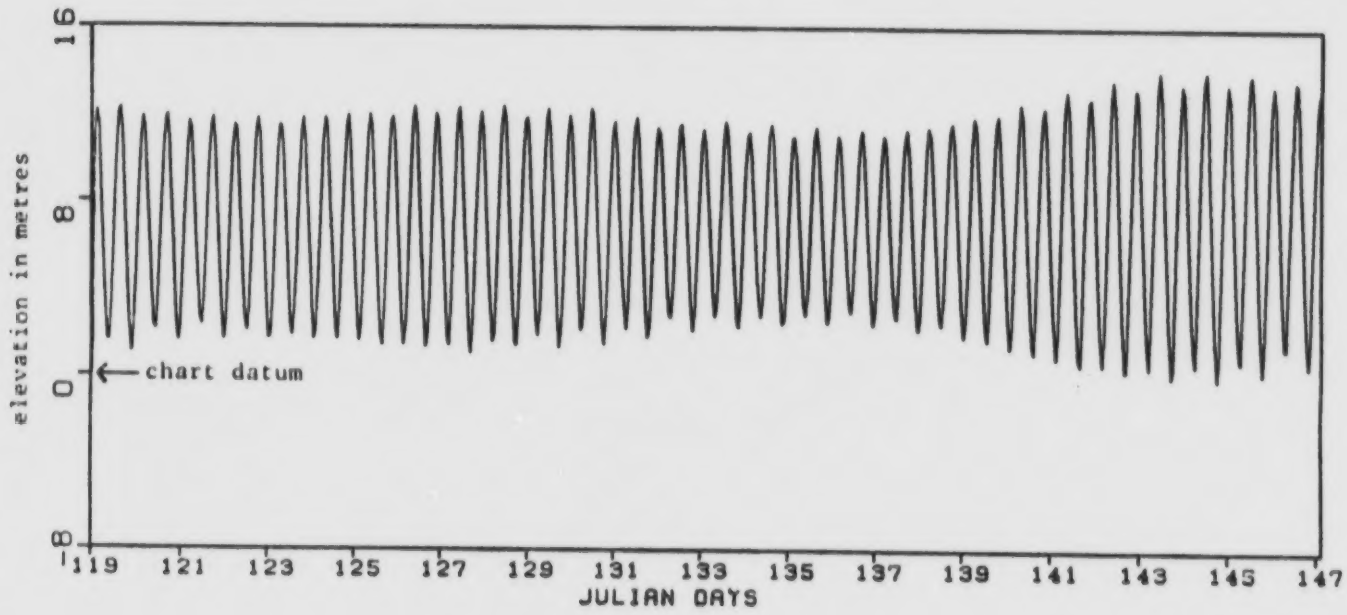

Figure 2-2 Plot of the 1986 tidal data recorded near Wood Point.

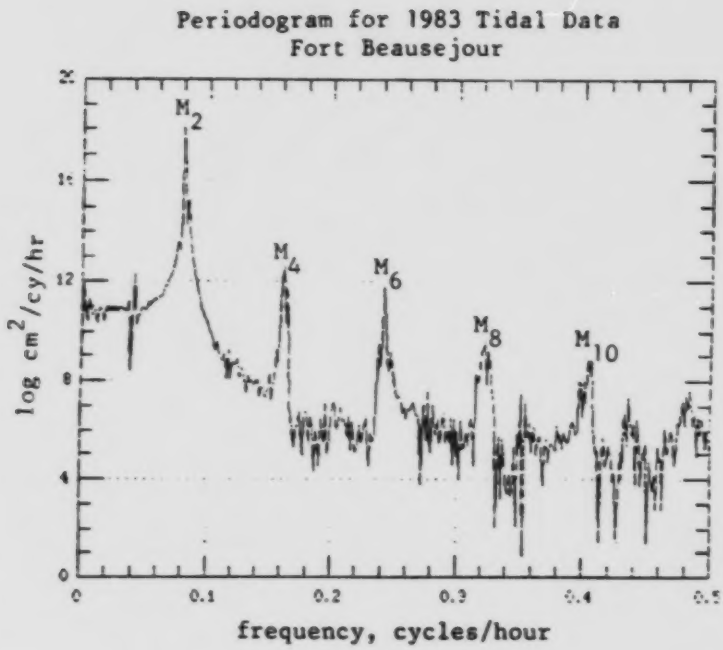

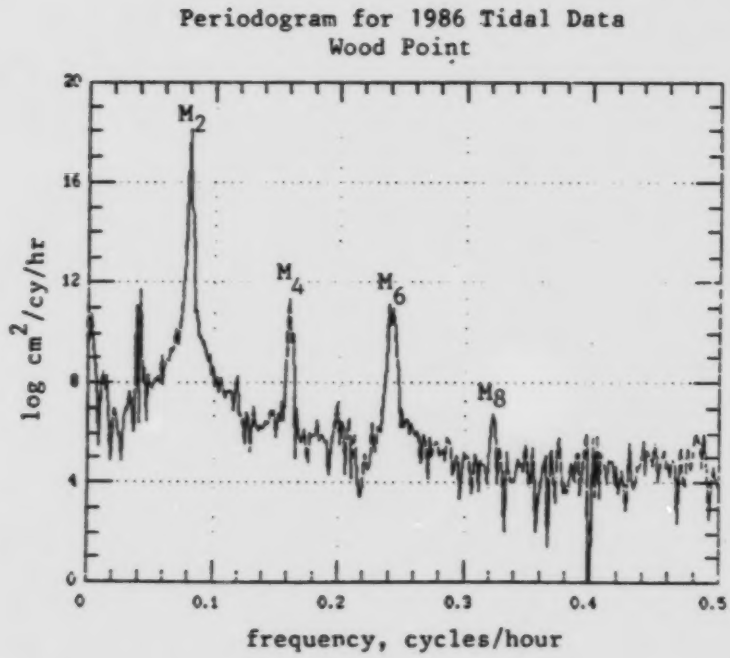

Figure 2-3 Periodograms of the Fort Beausejour (1983) and Wood Point (1986) tidal data.

Table 2-2. Amplitude and phase lag of the tidal constituents obtained from the least-squares harmonic analysis of the bottom pressure record observed in April - May 1986

Location: Wood Point (1986)
45 49.4 N 64 22.8 W
Large tide range: 14.6 m
Mean tide range: 10.9 m

Constituent	ampl (m)	Phase (deg)(Z+4)	Constituent	ampl (m)	Phase (deg)(Z+4)
Z0	7.000	.0	MM	.077	333.4
			MSF	.119	76.0
ALP1	.012	93.0	EPS2	.043	47.7
2Q1	.010	148.8	2N2	.058	295.4
Q1	.027	140.2	MU2	.020	82.0
O1	.126	125.0	N2	1.092	327.9
NO1	.034	179.3	NU2	.251	329.8
P1	.057	142.5	M2	5.098	351.1
K1	.163	141.6	L2	.245	354.8
J1	.013	160.2	S2	.783	35.8
OO1	.008	181.7	K2	.223	33.9
UPS1	.009	64.0	ETA2	.038	258.6
MO3	.019	225.5	MN4	.107	222.0
M3	.005	100.1	M4	.198	236.7
MK3	.003	324.6	SN4	.015	130.8
SK3	.009	119.6	MS4	.072	267.9
			S4	.004	310.7
2MK5	.017	68.3	2MN6	.170	351.3
2SK5	.009	346.8	M6	.196	2.9
			2MS6	.103	43.3
			2SM6	.015	80.9
M8	.014	194.9	M10	.003	28.6

Table 2-3 Amplitude and phase lag of the tidal constituents obtained from the least-squares harmonic analysis of the bottom pressure record observed in August - September 1983, by Mt. Allison University.

Location: Fort Beausejour (1983)
45 50.9 N 64 17.9 W
Large tide range: 13.8 m
Mean tide range: 10.6 m

Constituent	ampl (m)	Phase (deg)(Z+4)	Constituent	ampl (m)	Phase (deg)(Z+4)
Z0	6.379	.0	MM	.126	142.1
			MSF	.108	12.5
ALP1	.010	210.4	EPS2	.078	35.7
2Q1	.008	154.4	2N2	.199	349.4
Q1	.030	124.4	MU2	.068	136.0
O1	.133	131.4	N2	.910	327.9
NO1	.010	331.9	NU2	.209	329.8
P1	.074	145.0	M2	4.905	358.3
K1	.212	144.1	L2	.671	40.6
J1	.015	165.3	S2	.711	40.6
OO1	.011	301.3	K2	.203	38.7
UPS1	.003	348.6	ETA2	.042	193.5
MO3	.013	78.7	MN4	.149	249.5
M3	.022	134.1	M4	.353	270.1
MK3	.006	334.0	SN4	.084	12.3
SK3	.008	205.0	MS4	.153	332.4
			S4	.005	148.2
2MK5	.010	68.7	2MN6	.087	1.4
2SK5	.007	168.6	M6	.180	47.4
			2MS6	.102	109.9
			2SM6	.008	159.5
M8	.062	319.6	M10	.024	201.4

3.0 TASK 2 - DEVELOPMENT OF THE HYDRODYNAMIC MODEL

3.1 Introduction and Objectives

A hydrodynamic model is to be used to evaluate the change in the hydrodynamic regime of Cumberland Basin resulting from the exploitation of tidal power for electricity production. In order to provide a reference point from which changes can be assessed, the first task is to implement a model reproducing the natural tidal circulation. Another purpose of simulating the natural circulation of the basin is to ensure that the numerical solutions reproduce observed hydrodynamic behavior. Given that this is the case, confidence may then be had that the model will correctly predict the circulation as modified by tidal power generation.

In this section of the report the equations embodying the physical laws governing the movement of water in Cumberland Basin and the numerical techniques used to solve them are briefly reviewed. The information characterizing the geometry and boundary conditions of the basin is introduced for the purpose of numerical simulations (model grid, bathymetry, tidal elevation at the mouth of the basin, etc.). The result of simulations for the M_2 tidal constituent is used to check model calculations against field data and undertake any necessary adjustments to ensure good agreement. Final simulations using several tidal constituents and spanning a fortnightly tidal cycle are used to complete the description of the natural tidal hydrodynamic regime of Cumberland Basin and to provide further comparison with observations.

3.2 General Hydrodynamic Considerations

Before undertaking a mathematical modelling study of Cumberland Basin it is instructive to consider the relative importance of various factors affecting its hydrodynamic behaviour. We are interested in considering the time variation and the mean component of flows, both of which can be important to the aquatic environment of Cumberland Basin. The equations of motion for a shallow, homogeneous body of water can be given by (see Gill, 1982 for example):

$$\frac{\partial u}{\partial t} + u\frac{\partial u}{\partial x} + v\frac{\partial u}{\partial y} + w\frac{\partial u}{\partial z} - fv = -g\frac{\partial \zeta}{\partial x} + \frac{\partial}{\partial z}(N_v\frac{\partial u}{\partial z}) + \frac{\partial}{\partial y}(N_h\frac{\partial u}{\partial y}) \quad (A)$$

$$\frac{\partial v}{\partial t} + v\frac{\partial v}{\partial y} + u\frac{\partial v}{\partial x} + w\frac{\partial v}{\partial z} + fu = -g\frac{\partial \zeta}{\partial y} + \frac{\partial}{\partial z}(N_v\frac{\partial v}{\partial z}) + \frac{\partial}{\partial x}(N_h\frac{\partial v}{\partial x}) \quad (B)$$

$$\frac{\partial u}{\partial x} + \frac{\partial v}{\partial y} + \frac{\partial w}{\partial z} = 0 \quad (C)$$

where x, y and z are the cartesian coordinates with z upwards
u, v and w are the velocities in the x and y directions
t is time
g is gravity
N_v and N_h are the vertical and horizontal eddy diffusivities
ζ is the water level with respect to the surface at rest
h is the water depth with respect to the surface at rest

Taking x to be oriented locally along the channel, we can apply the following scaling:

$X \simeq$ 30 000m - length of the basin
$Y \simeq$ 3 000m - width of the basin
$Z \simeq$ 10m - depth of the basin (same as h)
$T \simeq$ 7 000s - tidal period/2π
$1/f \simeq$ 10 000s - (Coriolis parameter)$^{-1}$
$Z \simeq$ 5 m - tidal amplitude
$N_v \simeq 0.02 m^2/s$ - ($0.06\ u_* h$, Fischer, 1979)
$N_h \simeq 0.06 m^2/s$ - ($0.26\ u_* h$, Csanady, 1973)

Begining with equation (C) where $w(\zeta)=\partial\zeta/\partial t$, using X, Y and Z for the length scale of velocity variations, with Z and T for the amplitude and time scales of water level variations, we obtain that u, v, and w must be of order 2m/s, 0.2m/s and $7\cdot10^{-4}$m/s respectively. Introducing these values in the place of their respective variables and derivatives in equations (A) and (B), we can evaluate the size of the various terms in the momentum equations. Numbering the terms from left to right we obtain the following (in units of m/s^2):

A1	$3\cdot10^{-4}$	B1	$3\cdot10^{-5}$
A2	$1\cdot10^{-4}$	B2	$1\cdot10^{-5}$
A3	$1\cdot10^{-4}$	B3	$1\cdot10^{-5}$
A4	$1\cdot10^{-4}$	B4	$1\cdot10^{-5}$
A5	$2\cdot10^{-5}$	B5	$2\cdot10^{-4}$
A7	$4\cdot10^{-4}$	B7	$4\cdot10^{-5}$
A8	$4\cdot10^{-9}$	B8	$4\cdot10^{-11}$

It is immediately evident that the horizontal diffusion terms (A8 and B8) are negligible. All other terms are of comparable magnitude, with the Coriolis term (A5 and B5) playing a minor role in the U equation and a dominant role in the V equation. Since the V component of velocity is an order of magnitude smaller than the U component we can conclude that coriolis will play a small but non-negligible role in Cumberland Basin hydrodynamics. In the along-channel direction (U equation) the acceleration term (A1) and the vertical diffusion term (A7) dominate. The pressure terms (A6 and B6) have not been evaluated because the length scale of elevation changes (ζ) are not constrained by the dimensions of the basin (X and Y). The pressure gradients will adjust to the hydrodynamic conditions to balance the other terms. In the cross channel direction we can expect B6 to be about $2 \cdot 10^{-4}$ m/s^2 since it is the only term that can balance the Coriolis force. In the along-shore direction the pressure gradient term can be expected to be of the same order of magnitude as the acceleration and vertical diffusion terms (ie 10^{-4}).

Not considered above are the effects of density variation in Cumberland Basin. Assuming that horizontal density variations have a length scale constrained to the dimensions of the basin, it can be estimated that density differences in the order of 30 kg/m^3 (σ_t=30) would be required to affect the tidal circulation. These certainly do not occur in Cumberland Basin.

The momentum equations are subject to the following boundary conditions at the surface and bottom:

$$N_v \frac{\delta u}{\delta z} = \tau_x/\rho \quad \text{and} \quad N_v \frac{\delta v}{\delta z} = \tau_y/\rho$$

where τ represents the x and y component of bottom stress at the surface and at the bottom. Using a velocity of 2m/s and a drag coefficient of 0.003 a typical bottom stress of 12 Pa can be computed which is much larger than typical wind stresses (about 0.15 Pa for 10m/s) so that tidal influences can be expected to dominate the current structure most of the time.

The above equations can be averaged in time and analyzed in a similar manner to look at the equations of motion for the residual flow. The result is that the driving terms in the residual equations of motion arise from the "tidal stress terms" (the average of terms 2, 3 and 4 in equations A and B), which are of order 10^{-4} m/s^2. These will be balanced by pressure gradient terms and vertical diffusion terms, which would imply residual currents in the along-channel direction in the order of 0.2m/s. The effect of stratification would remain small but wind stresses would however be more important for the mean circulation. Wind stresses are not considered in this study.

Wright and Loder (1985) have considered the factors influencing the internal structure for oscillatory flow in Chignecto Bay, near Cumberland Basin. Their analysis is applicable here. In Cumberland Basin, their parameters E and F, which represent the relative rates at which momentum is lost to bottom and redistributed internally by viscous forces, are equal to 1.4 and 10 respectively. According to their results the oscillatory flow will show significant vertical structure throughout the water column. Similarly, the mean residual flow which is driven by the tidal stresses will also be depth dependent. This is in agreement with the data presented earlier.

3.3 Mathematical Model Description

The basic equations governing the flow of water in Cumberland Basin can be given as follows:

conservation of water volume:

$$\frac{\partial u}{\partial x} + \frac{\partial v}{\partial y} + \frac{\partial w}{\partial z} = 0 \qquad 3.1$$

and conservation of momentum:

X component $$\frac{\partial u}{\partial t} + u\frac{\partial u}{\partial x} + v\frac{\partial u}{\partial y} + w\frac{\partial u}{\partial z} - fv = \frac{-\partial p}{\rho\,\partial x} + \frac{\partial}{\partial z} N \frac{\partial u}{\partial z} \qquad 3.2$$

Y component $$\frac{\partial v}{\partial t} + u\frac{\partial v}{\partial x} + v\frac{\partial v}{\partial y} + w\frac{\partial v}{\partial z} + fu = \frac{-\partial p}{\rho\,\partial y} + \frac{\partial}{\partial z} N \frac{\partial v}{\partial z} \qquad 3.3$$

Z component $$\frac{-\partial p}{\rho\,\partial z} = g \qquad 3.4$$

where x, y and z are the three cartesian coordinates,

u, v and w are the velocity components in each coordinate direction

t is time,

f is the coriolis parameter,

ρ is the density of water,

p is the hydrostatic pressure and

N is the turbulent vertical diffusion coefficient.

For the Cumberland Basin application it is readily shown that the effects of variations in the density, ρ, are negligible. With ρ set constant, equation 3.4 can readily be integrated from the bottom to the surface to obtain pressure as a function of surface elevation, ζ, and the pressure gradient terms in equations 3.2 and 3.3 (first right hand terms) can be replaced by $-g \frac{\partial \zeta}{\partial x}$ and $-g \frac{\partial \zeta}{\partial y}$. Equation 3.1 can also be integrated from bottom to the surface to obtain an equation for the surface elevation, ζ :

$$\frac{\partial \zeta}{\partial t} + \frac{\partial \overline{V}}{\partial y} + \frac{\partial \overline{U}}{\partial x} = 0 \qquad (3.5)$$

where $\overline{U}$ and $\overline{V}$ denote depth averaged velocities. Surface elevation, ζ, therefore replaces pressure, p, as a dependent variable and equation 3.5 takes the place of equation 3.4.

The vertical diffusion coefficient in these simulations is derived from standard boundary layer theory, and is given by:

$$N = k \, u_* \, z \qquad (3.6)$$

where $k = 0.4$ is the von Karman constant and u_* is the friction velocity. This scheme has the advantage of removing the necessity to specify the vertical viscosity profile as a model input parameter. It is realistic for conditions where the turbulent energy originates entirely from bottom friction and where the bottom boundary layer occupies the entire water column. The

latter is not strictly valid everywhere in Cumberland Basin and may result in an overestimate of eddy viscosity near the surface at certain times in the tide cycle. However, this is a region where there is very little vertical shear and where the viscous terms are small, so that the effect of this approximation is negligible.

The above momentum equations do not include horizontal turbulent viscosities. The justification for this lies in observations (Holloway, 1981) and theory (Fischer et al, 1979) showing that the principal mechanism for horizontal dispersion is vertical shear dispersion, which is explicitly considered in these equations as well as in the model. A small amount of horizontal viscosity (8 m^2/s) is however retained to improve numerical stability in the computations.

Several alternatives can be considered to represent the vertical structure of the flow. Common approaches consist of dividing the vertical coordinate into layers of thickness Δz, so that by defining the velocities u, v and w for each level, the vertical derivatives in equation 3.2 and 3.3 can readily be evaluated (Laevastu, 1974 and Leendertse et al, 1973 for example). For this work, a method introduced primarily by Heaps (1972) and extended by others is adopted, which consists of representing the vertical velocity profiles as a linear superposition of a set of basis functions (P_i where i = 0, 1, 2...). Representing the

dependent variables, u and v, in the above equations by truncated sums of these basis functions ($\sum U_i P_i$ and $\sum V_i P_i$) and applying the method of weighted residuals, a set of coupled equations for the coefficients U_i and V_i are obtained. These coefficients vary in space and time, and can be evaluated numerically. The implementation of this technique is close to that of Owen (1980) and Gordon (1982) and uses Legendre polynomials on the interval [-1, 1] for the basis functions, P_i. This requires a linear transformation of the vertical coordinate, z, so that the new variable has values of 1 at the surface and -1 at the bottom. Figure 3-1 illustrates the shape of the first six Legendre polynomials, P_0 to P_5, and one can imagine how these may be combined to approximate any arbitrary function. Several methods are available to evaluate Legendre polynomials (Abramowitz and Stegun, 1972), the following recurrence relationship being one of the simplest:

$$P_n(x) = \frac{1}{n} ((2n-1) \times P_{n-1}(x) - (n-1) P_{n-2}(x)) ,$$

with $P_0(x) = 1$, and

$P_1(x) = x$.

The resulting relationships for U and V still contain the time derivatives and horizontal space derivatives found in equations 3.1 to 3.4. These are solved using a finite difference technique. Integration is therefore carried forward in time in

equal increments or time steps, Δt. All quantities are represented on a regular horizontal grid with constant cell size, $\Delta x = \Delta y$, so that spatial derivatives are readily estimated. Figure 3-2 illustrates the cell structure together with the grid used for low resolution (Δx = 800 m) simulations of Cumberland Basin; a similar grid is used for fine resolution (Δx = 400 m) runs. As shown, a space staggered grid system is used, with horizontal velocities (u and v) specified on the boundaries of each cell and vertical velocities (w) and surface elevations (ζ) specified in the center of each cell.

The vertical viscosity terms in equation 3.2 are solved in a time and space centered (implicit) manner which is unconditionally stable. The surface elevation (equation 3.5) and the pressure gradient terms in equations 3.2 and 3.3 are solved in a coupled, fully explicit, centered-in-space, forward-in-time method, and are subject to the Courant-Friedrichs-Lewy (CFL) stability criteria given by:

$$\Delta t < \frac{\Delta x}{\sqrt{2\ gh}}$$

This imposes a maximum integration time step of approximately 20 s for the coarse grid and 10 s for the fine grid in Cumberland Basin. The advective terms are solved using a Lax-Wendrof representation of the spatial derivatives and a five point average, forward in time approximation for the multiplier, as

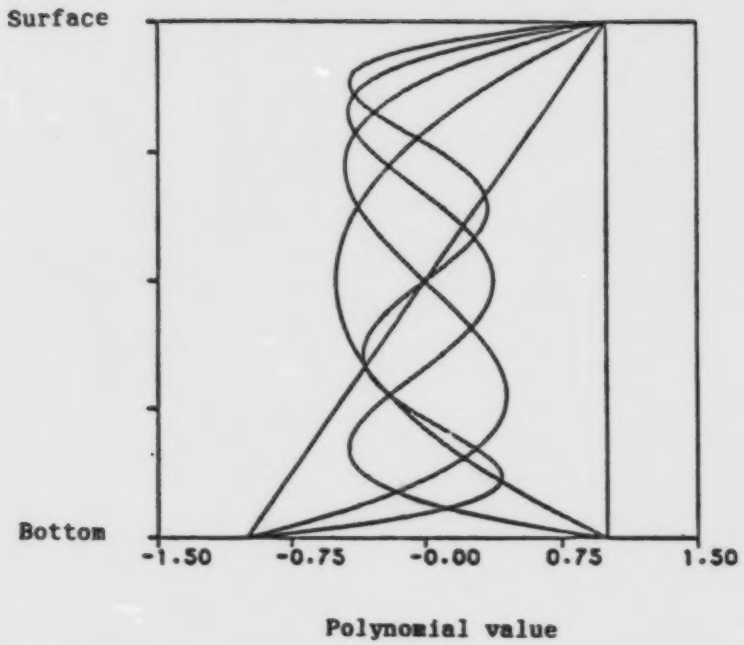

Figure 3-1 Legendre polynomial representation of the vertical structure.

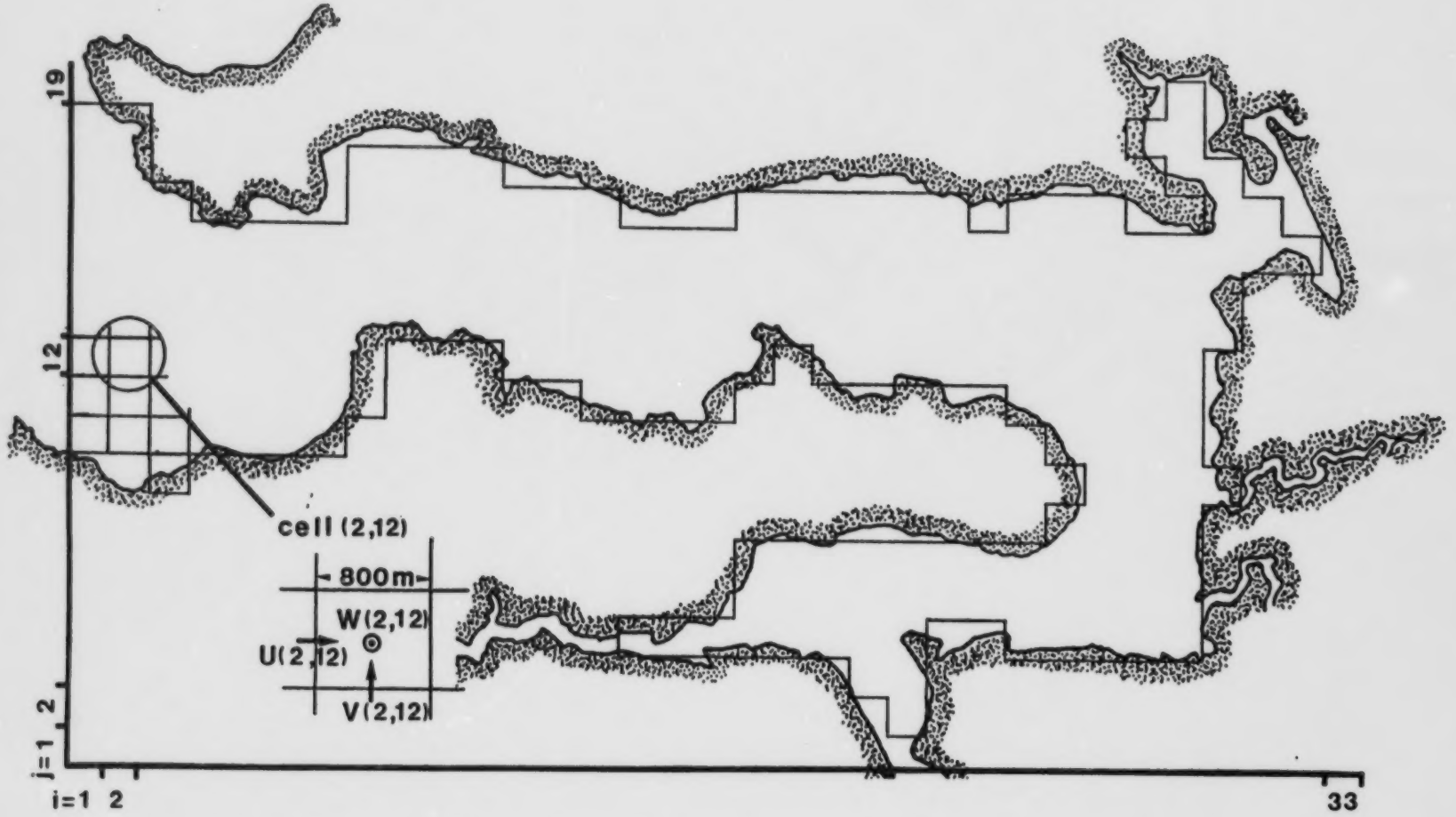

Figure 3-2 Coarse grid model and model variable definition sketch.

found in Mitchell and Griffiths (1980). This solution for the advective terms is stable as long as $\Delta x/\Delta t$ is less than the flow velocity. With maximum flow velocities of about 4 m/s this translates to maximum time steps of 200 s and 100 s for the coarse and fine grids respectively.

In order to take advantage of the stability of the viscous terms and advective terms for larger time steps, a time split integration technique is used. The continuity and pressure gradient terms are solved using the small time step dictated by the CFL condition with advective and viscous terms recomputed only once every 10 steps. This reduces computational requirements by an order of magnitude and tests have shown no significant effect on model results.

The above equations are solved, subject to the following boundary conditions:

- no flow is allowed normal to the coastline and to the bottom,
- water elevations are specified along open ocean boundaries, and
- the bottom stress is specified by a quadratic drag law.

The latter can be formulated as follows:

$$N \frac{du}{dz} = C_d u \sqrt{u \cdot u + v \cdot v}$$

where C_d is the drag coefficient.

This is preferred over a non-slip boundary condition for computational simplicity (Owen, 1980). The friction velocity used to specify N is given by $u_* = u_{-h} \sqrt{C_d}$. This parameterization is close to those of Wright and Loder (1985) and Tee (1979) where it is assumed that a thin constant stress boundary layer exists below the interior of the fluid which has a constant or depth dependent eddy diffusion coefficient.

3.4 Bathymetry

The sources of bathymetric data consisted of all available soundings for which there was an accurate position. These soundings have been collected by a variety of agencies since 1860, as summarized below:

Field sheet #	Agency	Year	# of soundings
D5313	British Admiralty	1860	1395
14	Canadian Hydrographic Service	1908	779
4090	Canadian Hydrographic Service	1965	1391
4776	Canadian Hydrographic Service	1978	1043
4777	Canadian Hydrographic Service	1978	467

Only field sheets are used since they are the primary source of data from which bathymetric charts are derived after a certain

amount of interpretation and adjustment. This is particularly important because of the changes in both the horizontal datum and the vertical datum over the years. Bathymetry was also taken in 1968 in support of tidal power studies, but was not available to the project.

All of the soundings from the above field sheets and within the model boundaries were digitized and entered into a computer database in the form of latitude, longitude and water depth. The latitude and longitude were recorded to an accuracy of 0.0001 degrees, which is equivalent to a resolution of about 11 metres of latitude and about 8 metres of longitude. The depths are recorded to 0.1 metre. In this database of 5075 soundings, the bathymetry is related to geographical position, rather than a specific model grid cell. This grid-free representation makes it suitable for use for any choice of grid size and orientation.

Before the soundings in the database could be used to form the model bathymetry, it was necessary to make adjustments to both the position and depth of the bathymetric database. The adjustments were as follows:

Vertical Adjustments:

The soundings from the various sources are not referred to the same vertical datum; the definitions of sounding and chart datum having changed over the years. Moreover, there has been

movement of the mud banks. As a consequence, adjustments to the soundings were necessary in order to bring them to a common vertical datum (Canadian Hydrographic Service chart datum).[1] It was possible to make some of the adjustments simply by comparing the elevations of known points on different sheets. Other adjustments were not so obvious, and were computed by making statistical comparisons of soundings grouped by field sheet, to evaluate datum changes in regions of relatively flat bottom, where the bathymetry is expected to be stable. As a result of these adjustments, all bathymetry is referred to the Canadian Hydrographic Service lowest normal tide datum, or chart datum.

Horizontal Adjustments:

In the late 1920's the geographical co-ordinate system of North America was adjusted. As a result, the geographical positions of the soundings on the 1860 and 1908 field sheets have shifted. Additional horizontal errors were introduced in the local determination of latitude and longitude and later corrected during chart preparation. For the 1860 and 1908 data, the following adjustments were applied:

Field Sheet	Latitude	Longitude	Adjustment
D5313	0.0003°	0.0008°	subtract
14	0.0007°	-	add

1 The relationship of chart datum to the Geodetic Survey of Canada is a function of the tidal range, and in the Cumberland Basin it is about 6.5 m below GSC datum.

Model Bathymetry

The depth of each model cell is determined by computing the average value of all soundings within the cell boundary. In addition to averages, the standard deviations are also computed for each cell, allowing an assessment to be made of the accuracy to which the model resolves bathymetric features.

Since many of the tidal flats in Cumberland Basin still remain unsounded, many model cells remain with undefined depth. For those cells, depthswere estimated visually from the bathymetric charts and the field sheets, using adjacent soundings and the general shape of bottom contours as a guide. For the coarse grid model 25 (11% of all cells) such estimates were required, while the fine grid model required 207 (22% of all cells). Bathymetric contours obtained from the gridded bathymetry, using the fine grid digital data, are shown in Figure 3-3. The standard deviation of actual depth in each cell is typically 2.5 m for the coarse grid and 1.0 m for the fine grid. Comparing this to the tidal range (~ 10 m), which is the most important vertical length scale, it can be concluded that the fine grid model will provide a reasonable representation of the Cumberland Basin geometry for modelling purposes.

3.5 Boundary Conditions

Open Boundaries

In order to solve for the tidal circulation within Cumberland Basin, the water elevation must be specified at the mouth of the basin which corresponds to an open boundary in the model. The amplitude and timing of the tidal forcing at the open boundary are obtained from the nearby tidal stations as well as from previous numerical studies considering the whole of the Bay of Fundy (Greenberg, 1979). These boundary conditions are expressed in terms of amplitude and phases for various tidal constituents, and are listed in Table 3-1. These are the principal tidal constituents and will reproduce the characteristic fortnightly cycle in tidal amplitude. Other constituents represent less than about 1% of the tidal energy arriving at the mouth of the basin.

Table 3-1 The amplitude and phase of the tidal constituents used on the open boundary of the model for the simulation of the fort-nightly tide.

Constituent	period (hr.)	amplitude (m)	phase (deg.)
Z_0	∞	.000	0.0
O_1	25.82	.132	120.2
K_1	23.93	.164	135.2
N_2	12.66	.832	321.4
M_2	12.42	4.780	350.9
L_2	12.19	.482	340.8
S_2	12.00	.714	31.5

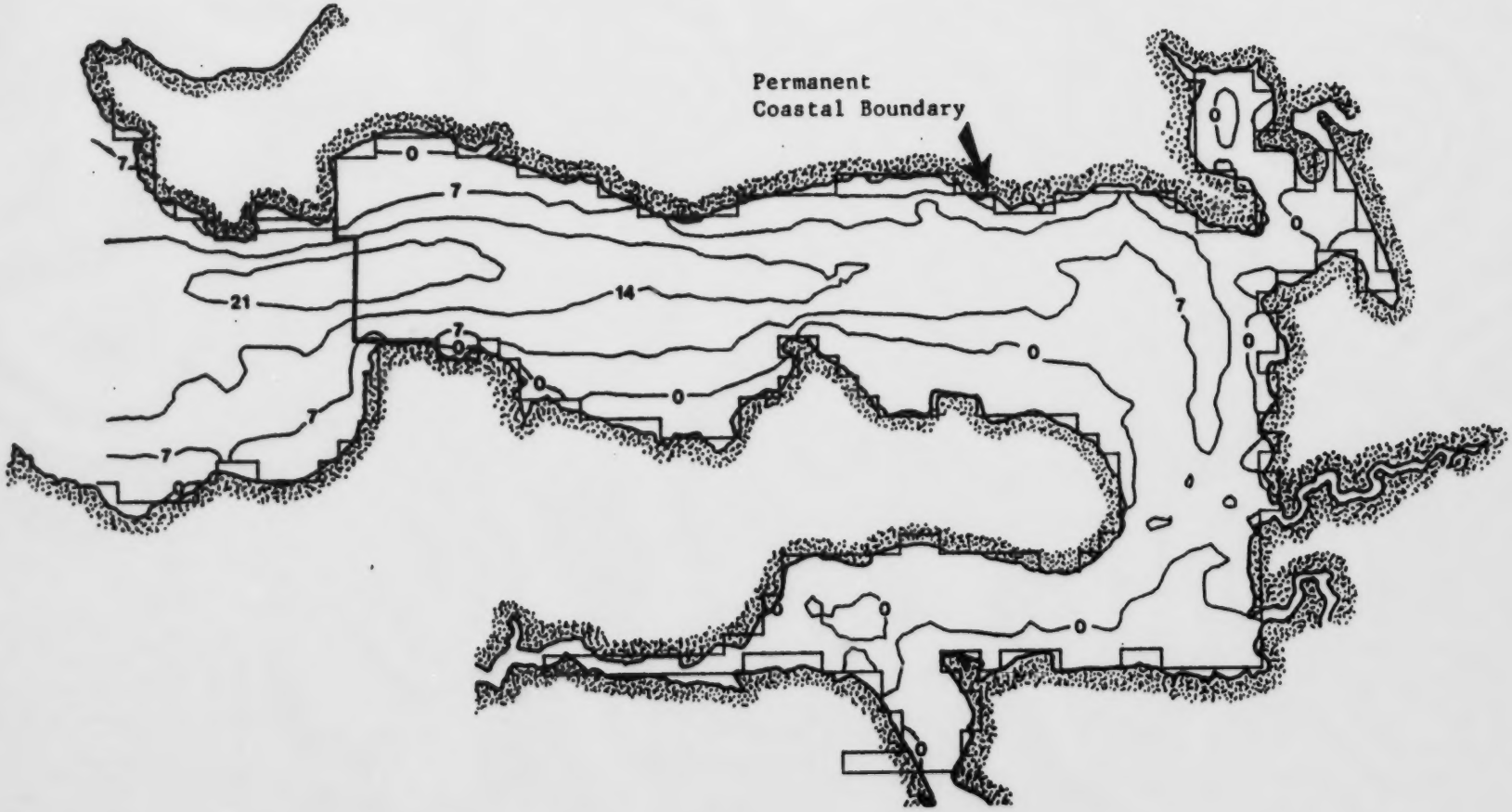

Figure 3-3 Fine grid model and bathymetry. Contours are in meters below mean sea level. The A8 barrage is indicated as a wide solid line.

Coastal Boundaries

As mentioned earlier a "no-flow" condition is imposed normal to coastal boundaries. Returning to the model grid system presented in Figure 3-2, it can be seen that this can readily be accomplished by setting the appropriate velocities to zero along the sides of cells adjoining a land boundary. Any cell in the model domain for which more than half of the surface area is above the higher high water line is defined as a permanent land boundary. In order to conserve computer resources, no storage or computation are used for cells which are entirely land. Permanent coastal boundaries have been indicated for the coarse grid and fine grid in Figures 3-2 and 3-3 respectively.

In the case of Cumberland Basin, coastal boundary conditions are complicated by the fact that almost half of the model cells represent tidal flats which may be dry and act as land boundaries at some time in the tidal cycle. In order to accommodate this, the water depth along the sides of every cell is checked at each integration time step, and the corresponding velocity is set to zero if the cell dries. In this way the coastal boundary conditions are determined dynamically at each time step.

3.6 Calibration

The only free parameter in the model is C_d, the bottom friction coefficient, which determines the rate of energy loss to friction. The principal effect of friction on tidal propagation is a retardation and attenuation of the signal (increase in phase

lag and decrease in amplitude). Because of the relatively small size of Cumberland Basin compared to the tidal wave length, phase lag variations are very small and the effects of bottom friction are expected to be difficult to detect. This is confirmed by model results illustrated in Figure 3-4 showing a cotidal chart obtained from simulation of the M_2 constituent, with very small differences in phase along the basin. The low sensitivity to friction has been verified by model runs using the coarse grid and the M_2 tidal constituent only, with drag coefficients, C_d, of 0.003 and 0.006, which show amplitude differences of 1% and phase changes of about four degrees at the location of the tide gauge. These quantities approach the resolution of the observations so that a fine tuning of the friction coefficient becomes pointless. A value of C_d= 0.003 was adopted for all subsequent model runs.

3.7 Verification

The model was run with a pure M_2 tide specified at the open boundary. The results were then analyzed for M_2 amplitude and phase by the Fourier analysis of one tidal cycle. The results of the analyses at points at which tidal data are available are shown in Table 3-2.

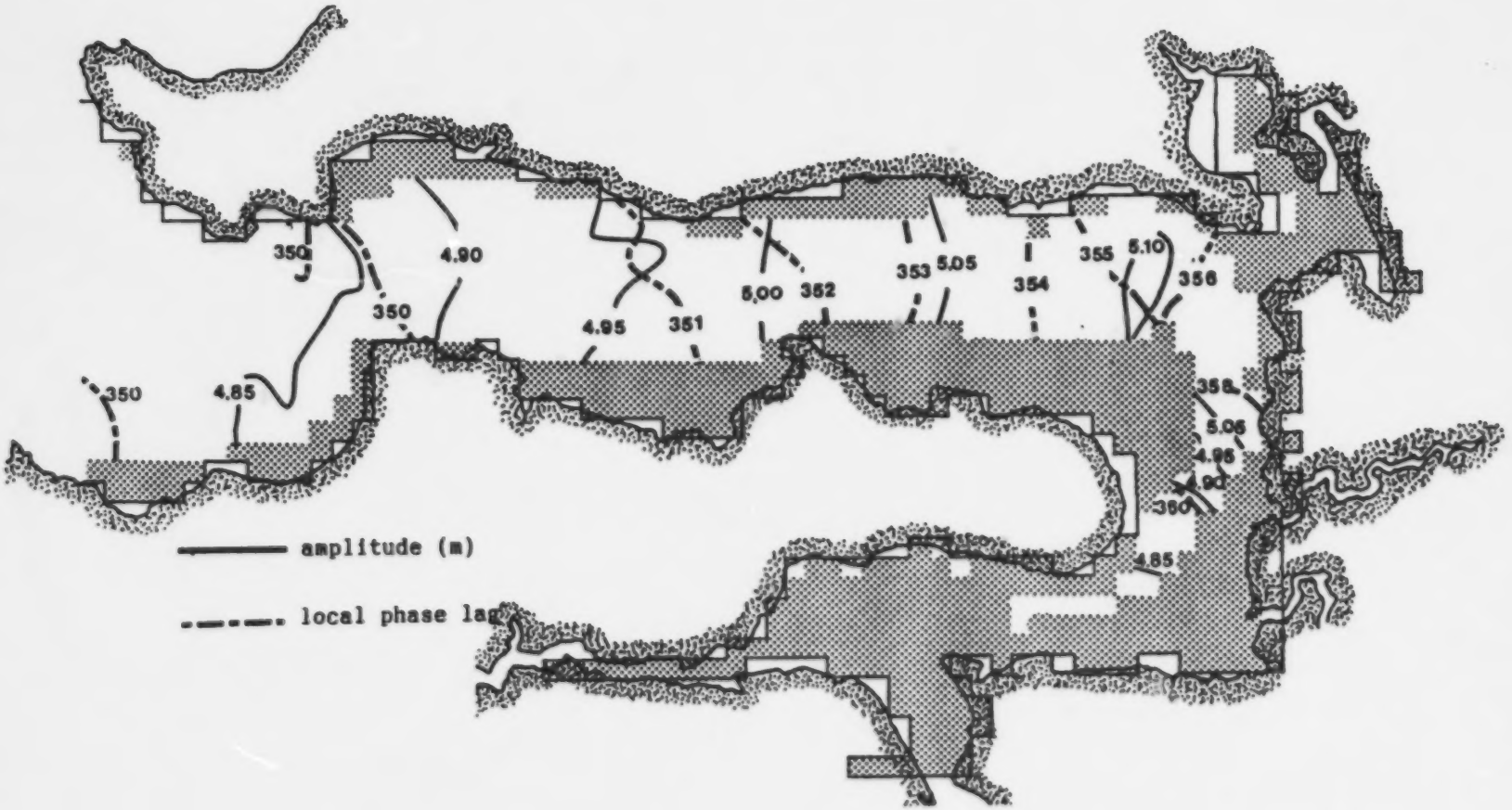

Figure 3-4 M2 cotidal chart for natural conditions.

Table 3-2 Agreement between the fine grid model and observations, for the M_2 tide. The amplitudes (h) are in metres and the phase (g) is in degrees relative to time zone GMT-4.

Location	Lat.	Long.	model(1) h	model(1) g°	obs(2) h	obs(2) g°	difference (2)-(1) h	difference (2)-(1) g°
Joggins	45.6963	64.4605	4.82	350	4.87	351	.05	1
Pecks Pt. 1986	45.7408	64.4983	4.85	350	4.71	350	-.14	0
	45.8233	64.3808	5.07	354	5.10	351	.03	-3
Mt.A(1983)	45.8478	64.2978	4.93	359	4.90	358	-.03	-1

An inspection of the above table shows good agreement between the observed and modeled M_2 tide. Except at Peck's Point, the differences in amplitude are 5 centimetres or less. The phases are all within 3 degrees, or about 6 minutes in time. The difference of 14 cm. in the amplitude of the M_2 tide at Pecks Point is not consistent with the general amount of error of the model. Reviewing the data, the value of 4.71 metres for the M_2 amplitude at Pecks Point could be low because of the difficulty of obtaining accurate tidal observations in the Pecks Point area with the equipment available in 1965, and the fact that it is not consistent with the other observations in the area.

It is interesting to note that the model correctly depicts the attenuation due to friction of the M_2 amplitude at Fort Beausejour.

The results of the model further up the basin are depicted in Figure 3-5. In this figure, the model output (from the

fortnightly run to be discussed in section 3.9) is compared with tidal observations taken at Minudie wharf (Cant 1986). The substantial distortions of the tidal curve (rapid rise, slow fall) that are typical in the upper reaches of an estuary are well represented by the model.

For most applications (Greenberg 1979; de Margerie and Lank, 1986) an agreement within a few percent is considered acceptable. The comparisons between the model and tide gauge observations are very good (Table 3-2) This, however, is not surprising given the small differences in phase and amplitude over most of the area of Cumberland basin where data are available.

3.8 Sensitivity Analysis

A sensitivity analysis was undertaken to ascertain that model results are not unduly affected by the choices of grid size, vertical resolution, formulation of the vertical viscosity profile, bathymetry, and thefriction coefficient. In order to minimize computational requirements, the base case for the sensitivity analysis uses the coarse grid model. The base case used a friction coefficient, C_d, of 0.003, a linear eddy viscosity profile scaled to the instantaneous bottom shear velocity (equation 3.4), a 6 polynomial representation of the vertical structure, and the best estimate of bathymetry (described in section 3.4). It should be noted, however, that the full

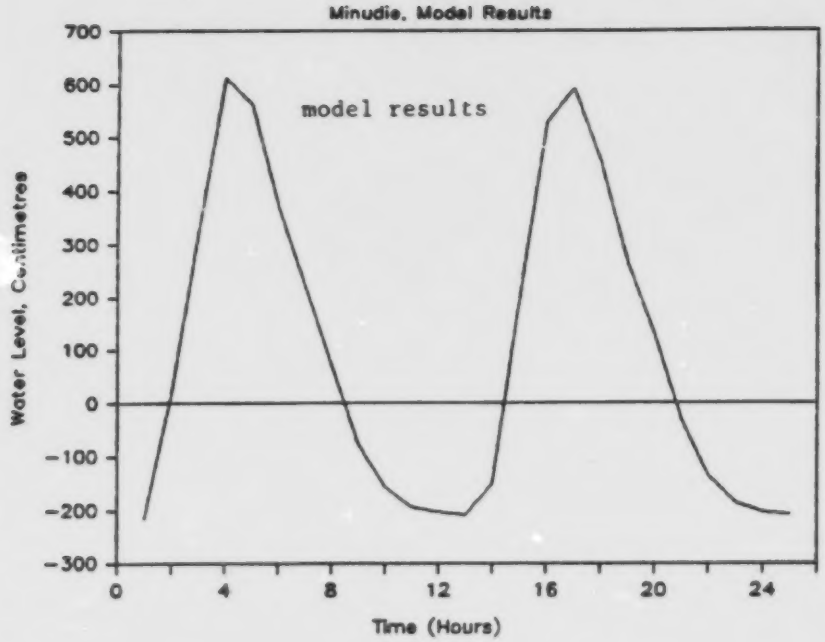

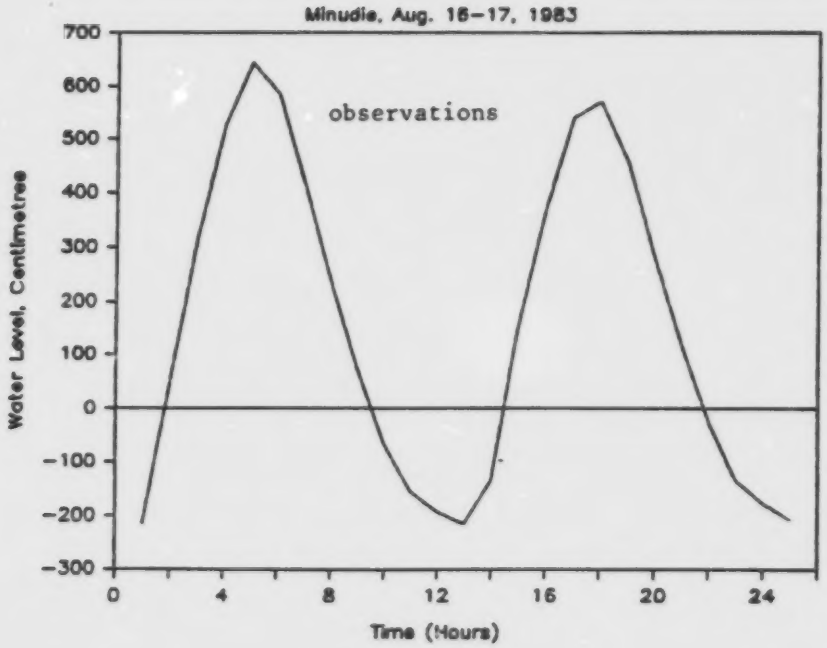

Figure 3-5 Comparison of model results with observations at Minudie wharf.

number of polynomials is reduced to 3, 2 and 1, for depths less than 3 m, 2 m and 1 m respectively. This improves the performance of the model both from a stability and computational requirement point of view and has negligible repercussions in the deeper areas of the Basin. In shallow regions many bathymetric features (drainage channels, boulders, etc.) with vertical scales of 1 to 3 m are not resolved by the model, and a detailed representation of the vertical flow structure should not be expected.

For the sensitivity analysis, a total of 7 cases were run in addition to the base case. Perturbations for each of these runs consisted of:

- increasing the friction coefficient,
- using two alternate formulations for the vertical viscosity,
- systematically increasing the depth at all cells by 1 m,
- decreasing the maximum number of polynomials to 4 and 2, and
- decreasing the model grid size to 400 m.

The effect of these changes are presented in terms of M_2 tidal parameters for selected locations in Table 3-3. As can be seen, tidal elevations show very little sensitivity even to very drastic changes in computational parameters. The depth integrated currents similarly show very little dependence on model parameters. This behaviour is expected for a small basin, as the circulation will be dominated by the requirement of continuity.

The bottom velocity and bottom stress estimates are much more sensitive to the selection of the drag coefficient and vertical viscosity formulation. The dependence of the vertical velocity structure is also shown for the ebb tide in Figure 3-6 (results

are similar for other stages of the tide). This shows only moderate dependency of the velocity profile on the parameterization of the eddy diffusivity. These results are in agreement with Wright and Loder (1985) and Tee (1982) which shows little dependence of the velocity profile on the specified function for the eddy diffusivity profile. It is worth noting that the 3-D formulation presents an advantage in that the bottom stress is less dependent on drag coefficient than would be expected for a 2-D model. These results point to the importance of considering the vertical hydrodynamic structure for sediment transport studies which depend critically on bottom stress and on the current structure near the bottom. Depth dependency of the results is very small so that any error in the bathymetry of the basin would have a negligible effect.

As seen from the sensitivity analysis, there is a difference, although small, in the results of the two grid sizes, confirming that the most important space scales are resolved, but that more precision is gained by using the fine grid. The solution with four polynomials is much closer to the base case than the two polynomial solution, indicating convergence of the solution. The 400 m grid size and 6 polynomial representation are near the limit of computational feasibility with large mainframe computers, requiring about 9 hours of CPU time to simulate one tidal cycle (12.42 hours) on a CDC CYBER 830 computer. These parameters were therefore retained for final model runs and tidal barrage simulations.

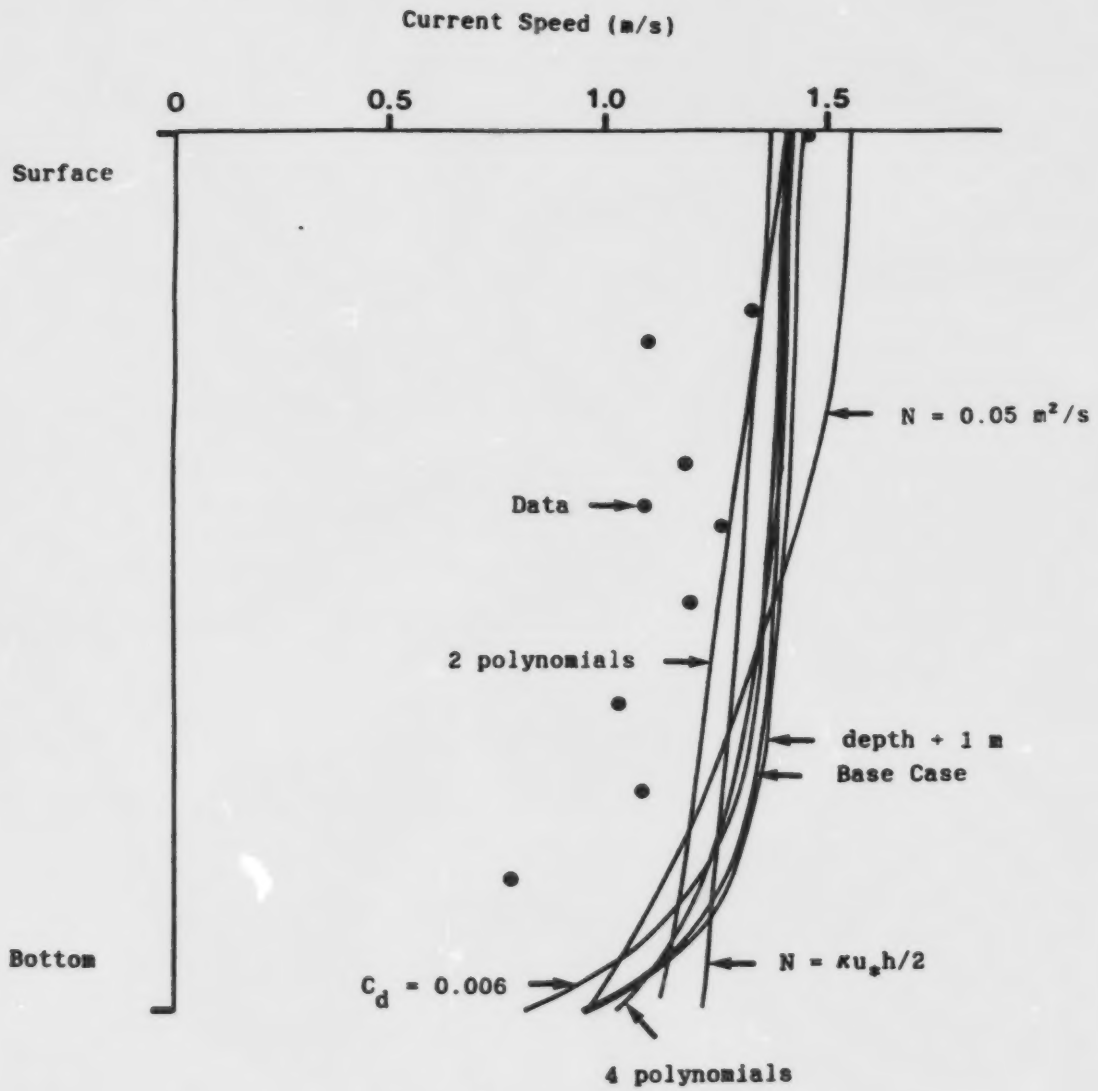

Figure 3-6 Sensitivity analysis of the vertical velocity profile at ebb tide. Data points shown for comparison are for stations 1 and 2 in Hildebrand et al (1980), and are for a period of smaller tides (close to the neap tides), explaining the smaller mean velocity.

3.9 Simulation of the Fortnightly Tidal Cycle

Tides in the Bay of Fundy and Cumberland basin are dominated by the semidiurnal cycle usually characterized by the M_2 tidal constant. This semidiurnal cycle is however strongly modulated on a fortnightly cycle. Tidal ranges typically change by ± 30% over a fourteen day period. To a first approximation, tidal elevations and currents can be considered proportional to the tidal range, and the results of M_2 simulations (to be presented later) can be scaled, up or down, according to the actual range for a period of concern. Certain aspects of the circulations do not scale linearly with tidal amplitude and only a simulation undertaken over a fortnightly cycle can resolve them. These are the residual circulation and the bottom stress which depend on the square of the tidal range. These are crucial in assessing sediment stability and exchange rates between various parts of the Cumberland Basin.

The period from the first to the eighteenth of September1978 was used for the fortnightly simulations. This covers a period of spring and neap tides at a time when the lunar nodal modulation is at a maximum. Only the last fourteen days of simulations are used in any analysis, to allow for the settling of the model solution after starting from rest. The input at the open boundary consisted of a time series calculated from the constituents listed in Table 3-1. Figure 3-7 shows the normal tide range throughout Cumberland Basin with regions which dry for part of the tidal

cycle shaded. The results of this simulation are depicted in terms of mean scalar bottom stress for the fortnight (Figure 3-8) and the depth mean residual current over the fortnight (Figure 3-9). The mean bottom stress calculated from the fortnightly run is somewhat less than that calculated for M_2 alone. This is a sensible result, because the bottom stress scales with the variance of the tidal signal. The variance of a 14 day period of record is about eight percent less than M_2 variance, and the variance for a 29 day period is about seven percent greater. The mean bottom stress for the 29 day period may be estimated by scaling up the bottom stress for the M_2 and 14 day values.

TABLE 3.3

Sensitivity Analysis from M2 Simulations

Percentages shown are the relative changes in M2 amplitude due to parameter permutations.

Base Case	Permutation	tidal elevation (1986 gauge)	depth mean current (station 291)	depth mean current (station 290)	change in bottom current*	change in bottom stress*
drag coefficient						
0.003	0.006	+1%	-2%	-3%	-14%	+48%**
depth						
	+ 1 m	0%	-1%	-1%	-2%	-4%
number of basis functions						
6	2	-1%	-2%	-3%	+30%	+69%
	4	0%	-1%	0%	+9%	+19%
viscosity formulation						
linear	vertically uniform but scaled to the local friction velocity					
$\kappa u_* z$	$\kappa u_* h/2$	-1%	-2%	-3%	+27%	+60%
	constant					
	$\equiv 0.05\ m^2/s$	0%	+1%	0%	+9%	+19%
grid size						
800 m	400 m	0%	+8%	-8%		

* Bottom currents and stesses are computed for the ebb tide at station 290.

** A value of 100% would be expected from a 2-D simulation.

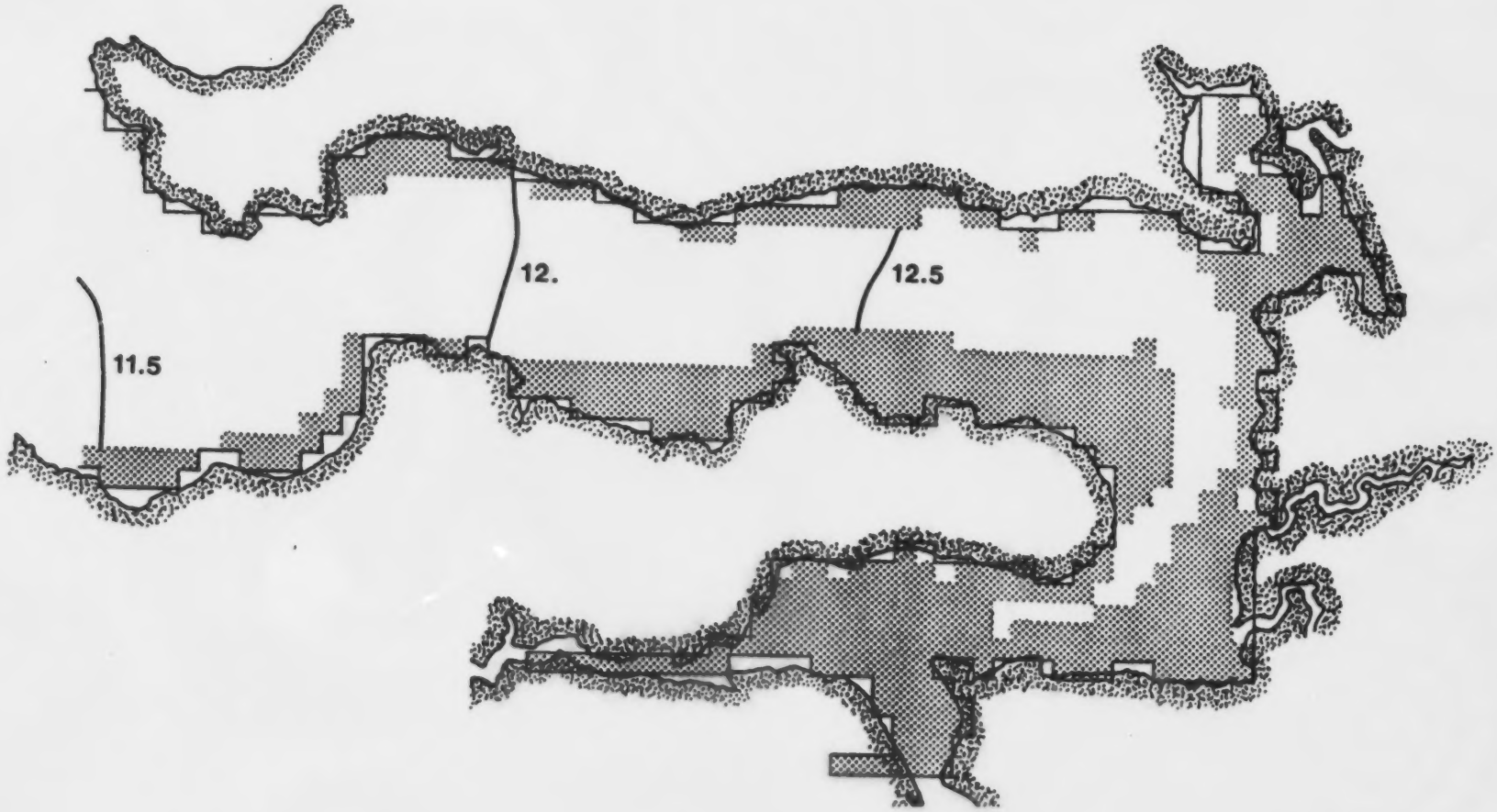

Figure 3-7 Tidal range computed from a fortnightly simulation (shaded area represent drying areas)

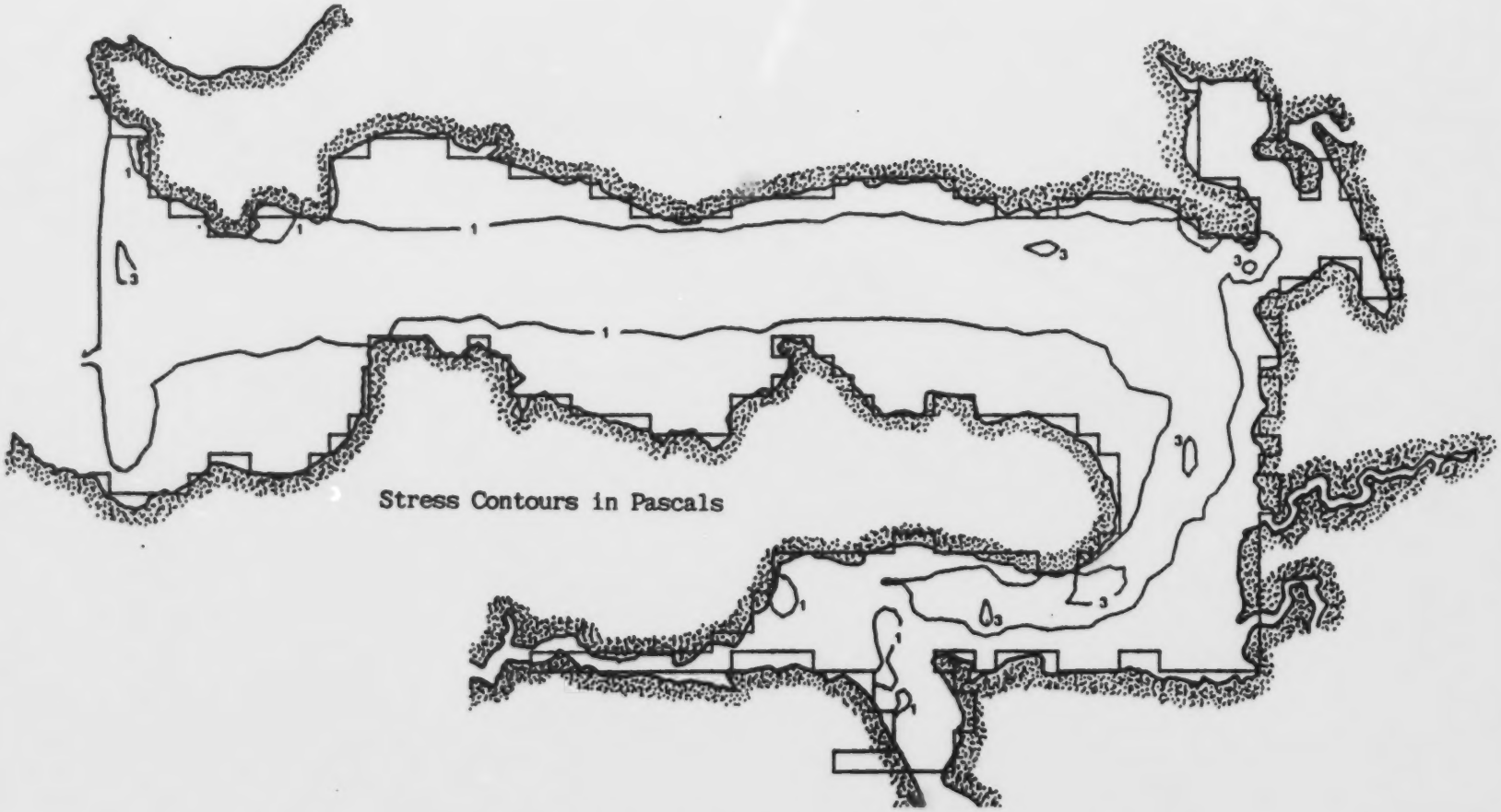

Figure 3-8 Mean bottom stress (scalar) from a fortnightly simulation

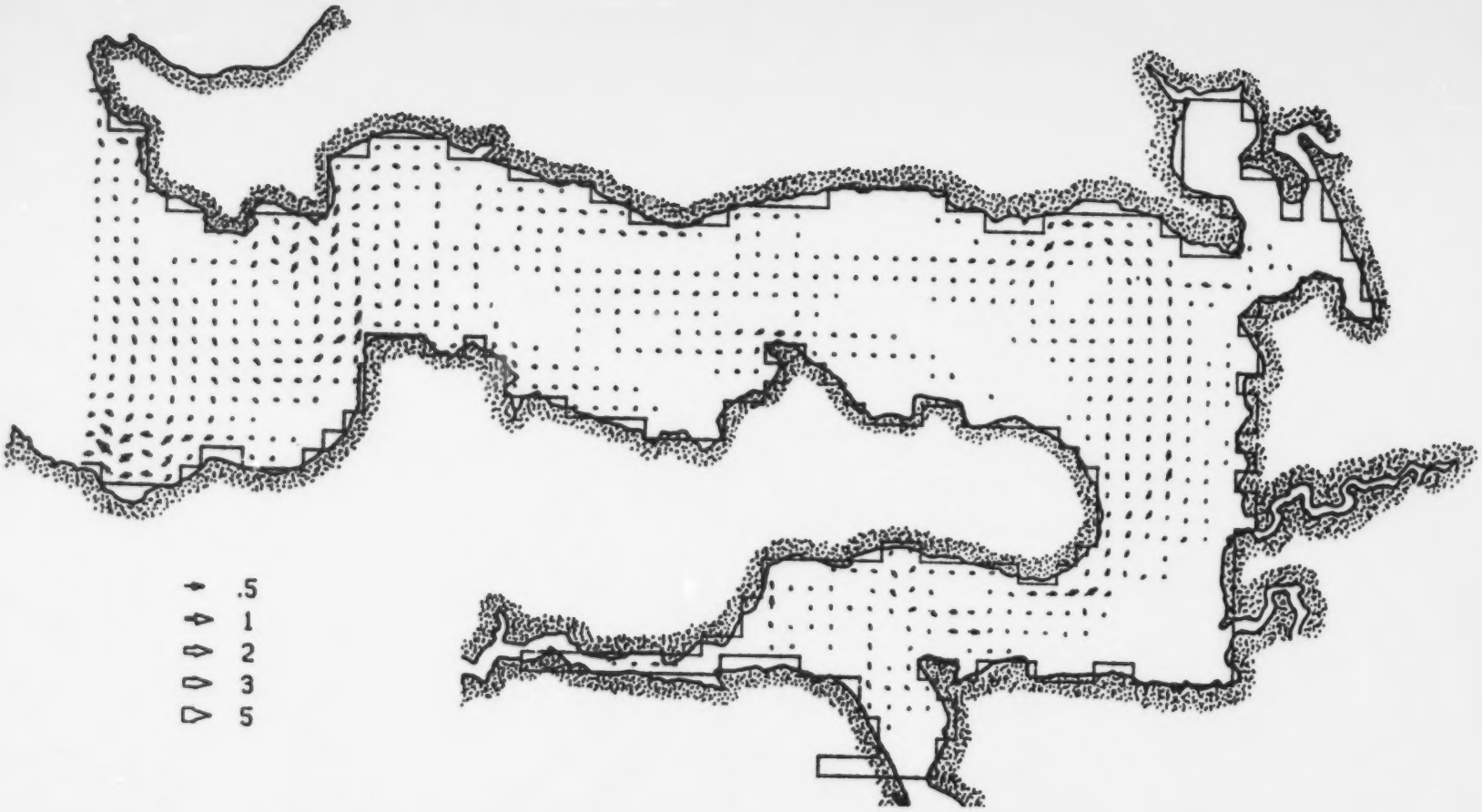

Figure 3-9 Depth mean residual currents from a fortnightly simulation

4.0 MODEL APPLICATIONS

4.1 Introduction

A final task of this project is to employ the 3-D hydrodynamic model developed and described in section 3 to make an assessment of the impact of the A8 tidal power project on the tidal regime of Cumberland Basin. For this application, the tidal barrage, location, and operating characteristics were incorporated into the model, for calculation of the barrage - induced modifications to both the tidal regime and the circulation patterns.

4.2 The A8 Barrage

The design of the A8 barrage for this study draws on the work of Tidal Power Consultants Ltd. (1984) and Discovery Consultants Ltd. (1985). In a study by Tidal Power Consultants Ltd. (1984), variable speed turbines were optimized for the A8 site. They had the following characteristics:

- output 34MW at 0.95 generator efficiency
- rated head 6.841 m
- flow of 665.13 m^3/sec at maximum output rated head

The flow characteristics of the A8 optimized generating routine are for a turbine operating on a maximum energy output schedule. The relationship between flow and head for this turbine is taken from the report by Discovery Consultants Ltd. (1985) and is reproduced in Figure 4-1. In order to describe these rather complicated head-dependent flow characteristics of this optimized generating routine, the complete curve was partitioned into four segments, each represented by a second order equation, except for segment 4 which was represented by a third order equation which followed the maximum power curve.

Table 4-1 The coefficients of the least-squares fitted equations and applicable heads.

Segment	from	to	Equation	max. error (%)
			Head increasing	
1	4.98m	6.32m	$Q = -1185 + 469h - 31.1h^2$	0.3
2	6.32m	max.	$Q = -249 + 249h - 19.6h^2$	0.3
			Head Decreasing	
3	max.	4.29m	$Q = 567 - 13.6h + 0.949h^2$	0.4
4	4.75m	1.50m	$Q = 169 + 103.0h - 4.800h^2 - .271h^3$	0.0

where h is the head in metres and Q is the flow in cubic metres/sec.

A barrage subroutine was written for the A8 barrage which incorporated the above specifications.

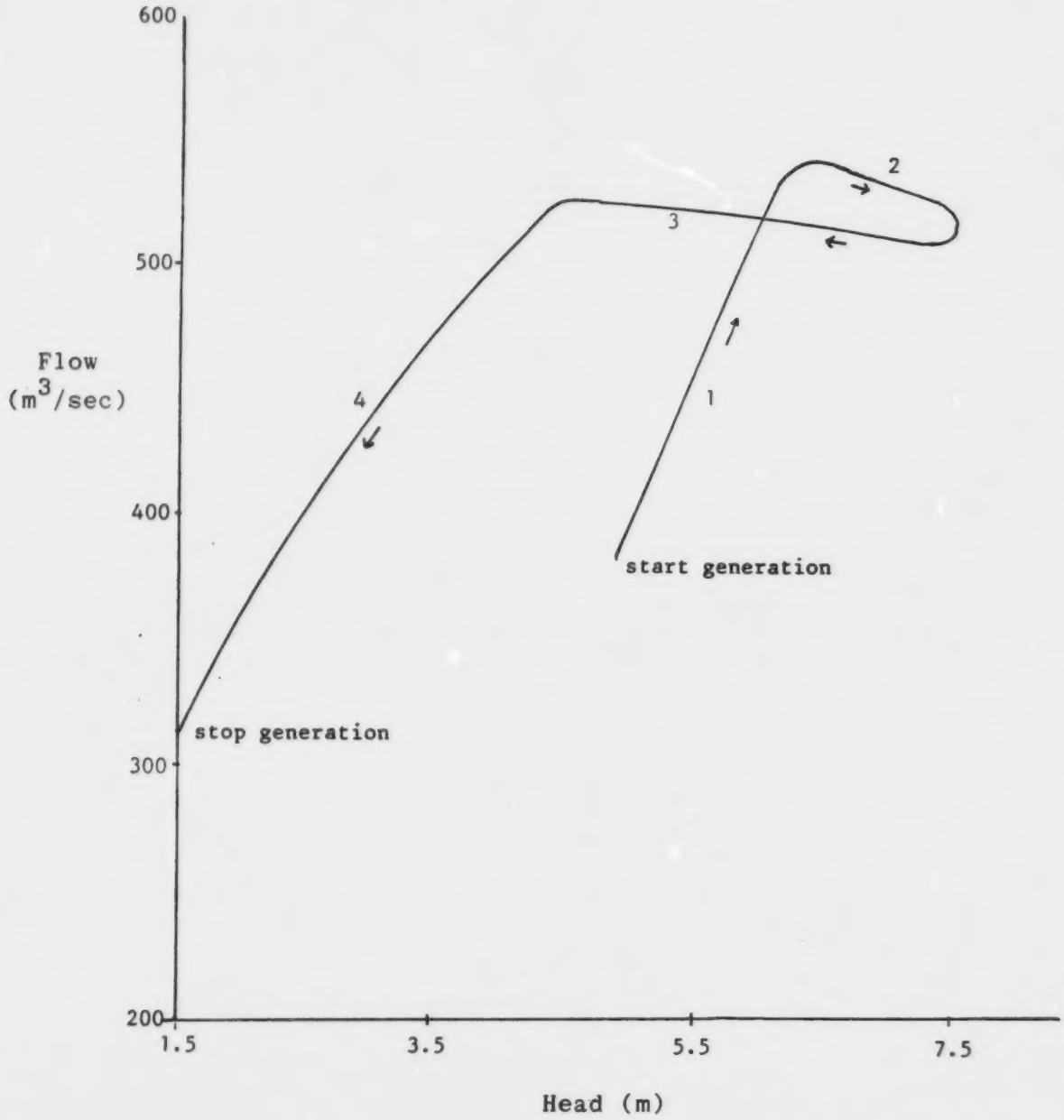

Figure 4-1 Flow characteristics of a single turbine at A8. The segments used for the fitting of the least squares equations are as numbered.

4.3 The Pre-Barrage Tidal Regime

Some of the results of the simulations of the fine grid model for the natural regime were discussed in section 3. In this section the description of the natural regime will be extended to include the additional model calculations of the mean bottom stress and the depth mean residual currents.

The bottom stress (Figure 4-2) is essentially evenly distributed throughout the basin. It is generally 1 Pa over the deeper areas and as high as 3 Pa in the middle of the channel. The residual circulation pattern is always below 0.5 m/sec except near the mouth of the basin where the presence of the model boundary may affect the accuracy of the solution. Mean circulation shows no net drift in or out of the basin but shows a complex system of eddies.

4.3 Barrier Operational Scenarios

There were two simulation runs made with the A8 barrage in place. The first simulation was a 'base' run in which the most up-to-date design concepts for the layout and operation of the A8 barrage were used. In the second production run, substantial changes in the placement of both the turbines and the sluices were incorporated, while retaining the overall geometry of the A8 barrage.

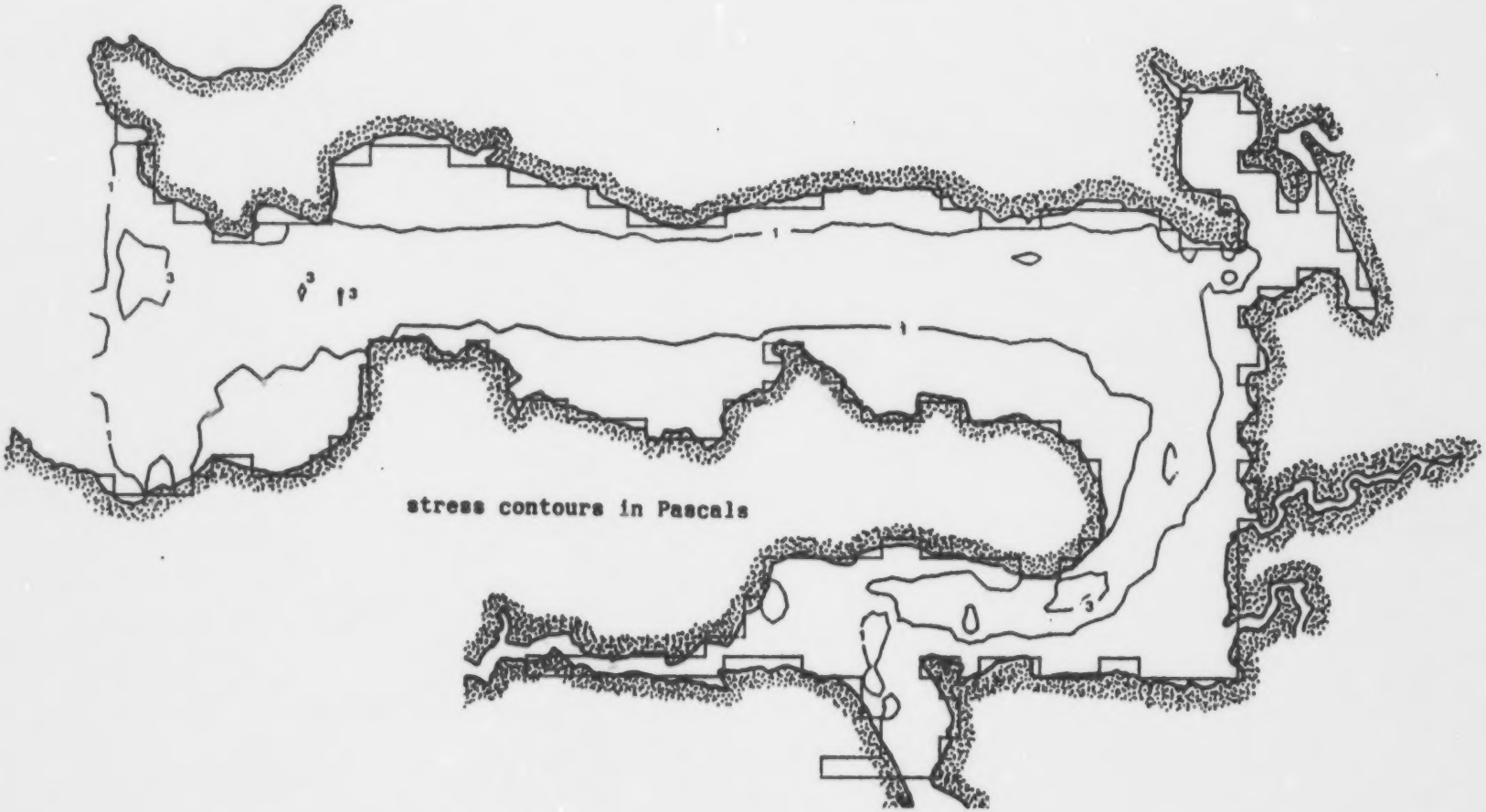

Figure 4-2 Mean magnitude of bottom stress (scalar) for the M_2 tide, under natural conditions

The configuration of the A8 barrage for the first production run closely approximates the A8 barrage as described in Fundy Tidal Power Update '82 (1982), using 35 operating turbines and 24 sluices. The 35 turbines were split between the two model grids closest to the actual location of the turbines. Seventeen turbines were placed in one grid cell and 18 turbines in the other. The 24 sluices were placed in one grid section. The rest of the barrage is an impermeable dyke. A discussion of the barrage specification data file and how to modify it is given in Appendix B.

4.5 The Post-Barrage Tidal Regime

The operation of a tidal barrage drastically alters the tidal regime in the headpond. A comparison of the pre-barrage and post barrage tidal regime is presented in Table 4-2.

Table 4-2 Comparison of the pre- and post- barrage tidal elevations in Cumberland Basin. The amplitude (h) and the phase (g) of M_2 are tabulated at a number of sites for both the natural tidal regime and the barrage modified regime.

Location	Lat.	Long.	before h(m)	before g(°)	after h(m)	after g(°)	difference h(m)	difference g(°)
Joggins	45.6963	64.4605	4.82	350	4.84	349	-.02	-1
1986	45.8233	64.3808	5.07	354	1.49	82	-3.58	-88
Mt.A(1983)	45.8478	64.2978	4.93	359	1.53	82	-3.40	-83

The mean value of the elevation of the headpond is about 3.2 metres everywhere.

A comparison of head pond mean level and M_2 amplitude was made between the results for Cumberland Basin with the Greenberg (1979) model, using a similar barrage arrangement (see Table 4-3).

Table 4-3 Comparison of mean head pond level and tidal amplitude for the present study, for Greenberg (1979).

Model	mean value (m)	M_2 amplitude (m)	M_2 phase (deg)
Present study	3.19	1.45	82
Greenberg (1979)	2.65	2.28	54

The values that the two models produce for the amplitude and phase of M_2 are quite different. This is attributable mainly to the difference in the volume of Cumberland Basin specified in the two models. Assuming an average depth, the ratio of the volumes of Cumberland Basin in the two models will be the ratio of their areas. For the Greenberg model the total area of Cumberland Basin is 87.6 sq. km. The present model of Cumberland Basin has a headpond surface area of 120 sq. km. The ratio of the areas is 0.73, and the ratio of the M_2 amplitudes is 0.64. The similarity of these ratios supports the argument that the differences in the M_2 tidal regime are due to the much better resolution of the area by the present fine grid model.

Another factor affecting the results may be the specification of the boundary condition at the mouth of Cumberland Basin. The tidal elevation at the mouth of the Basin depends to a degree on the response of the Basin itself. Since the presence of a tidal barrage significantly modified the response of the basin, it can be expected that the tidal elevation at the mouth will change. This depends on the interaction between Cumberland Basin and the Bay of Fundy as a whole and would be best considered by a coupled model of the two water bodies. This was not undertaken. Simulation of the whole Bay of Fundy including Cumberland Basin (Greenberg, 1979) suggests that the amplitude at the mouth should be reduced by approximately 0.28 m.

The current regime for the flood tide and ebb tide cases is shown in figures 4-3 and 4-4, and the regime for at low tide is shown in figure 4-5.

A view of the current regime in Cumberland Basin at low tide with the A8 barrage in position is shown in figure 4-6. Figure 4.7 depicts the current regime at high tide with the barrage in place.

With the barrage in operation the residual circulation in the upper basin is largely suppressed. Similarly, bottom stresses are drastically reduced upstream of the barrage. This is seen in figure 4-8 showing the difference in stress (natural minus

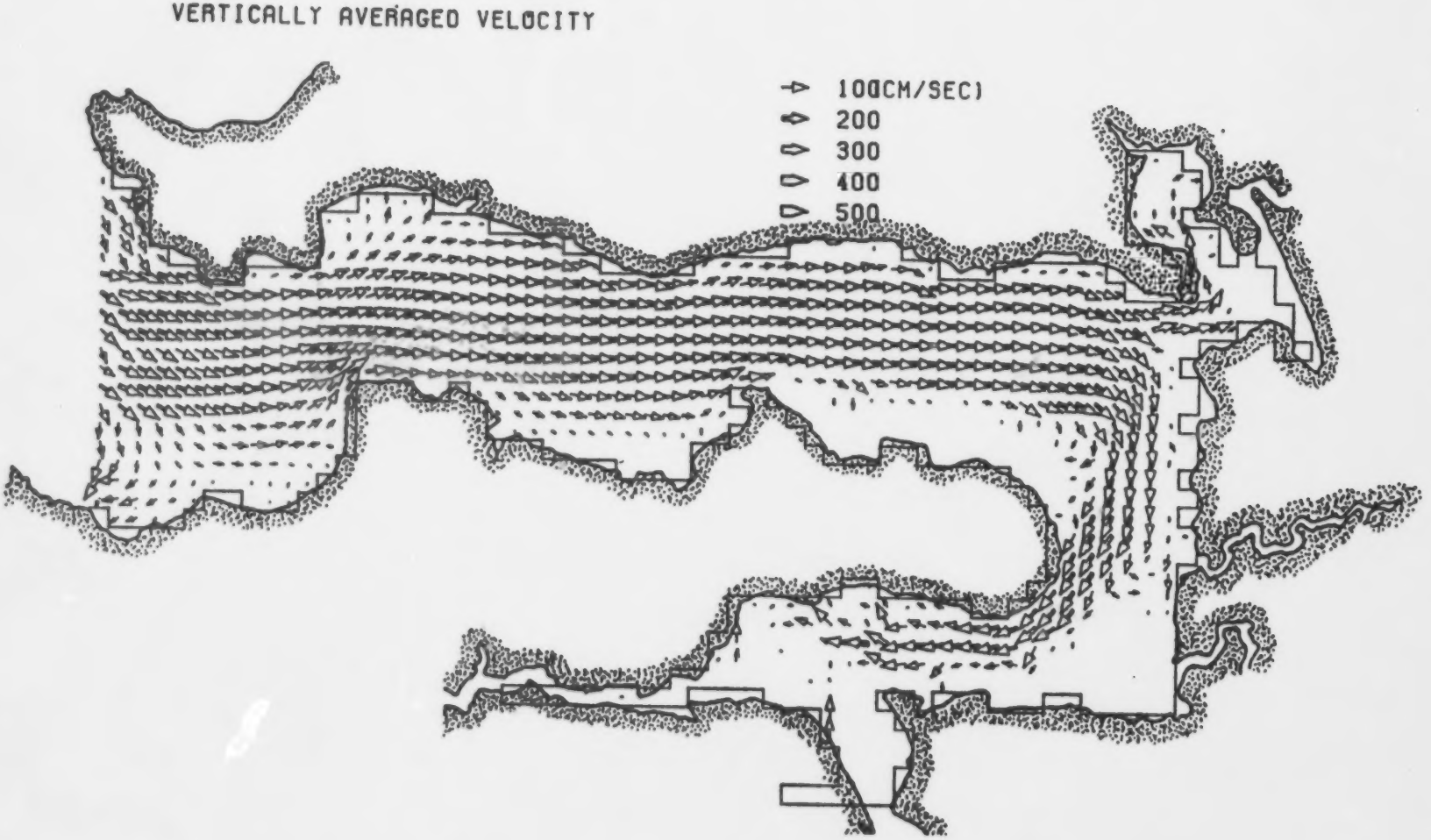

Figure 4-3 M_2 current regime at flood tide, under natural conditions

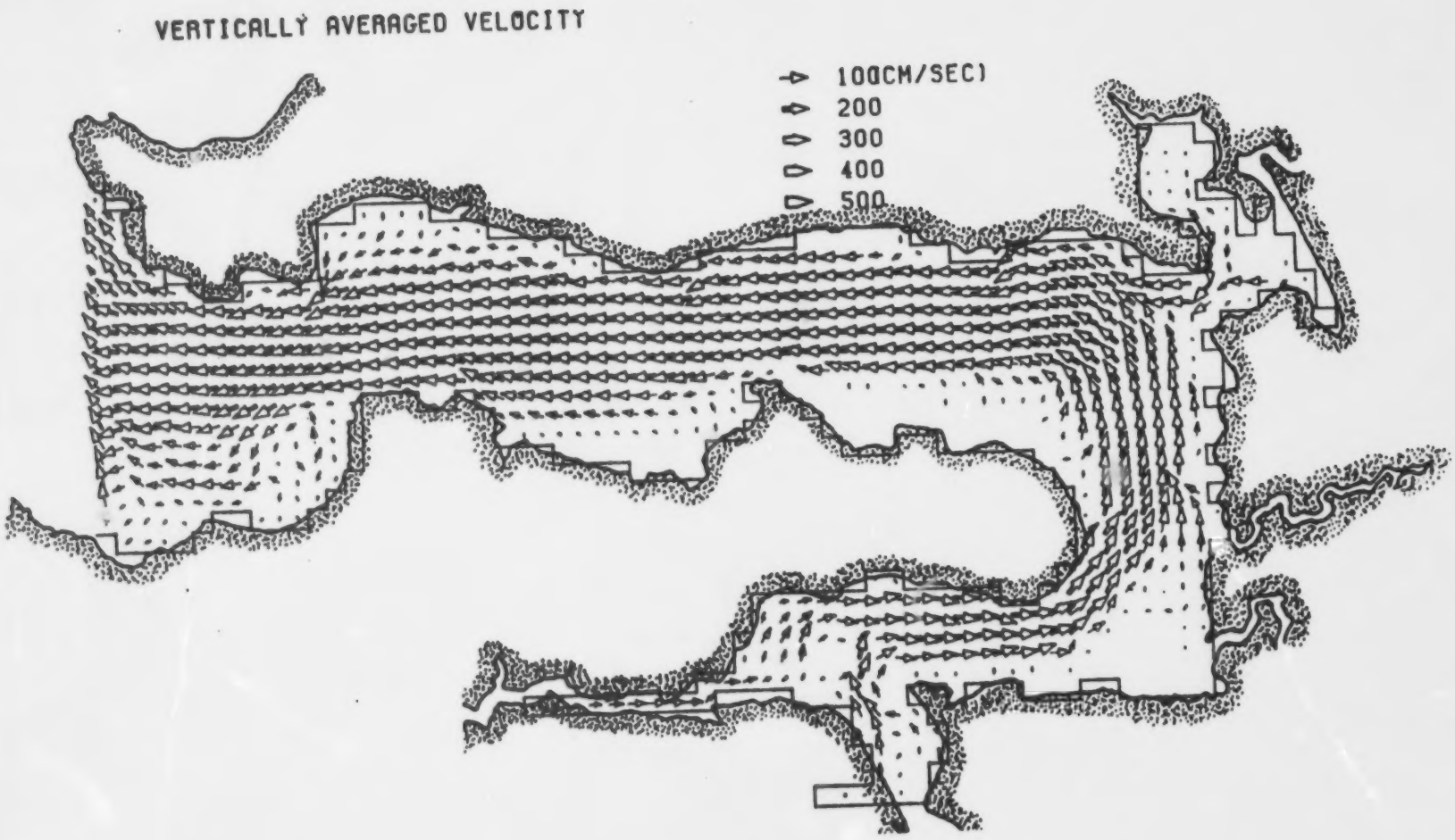

Figure 4-4 M_2 current regime at ebb tide, under natural conditions

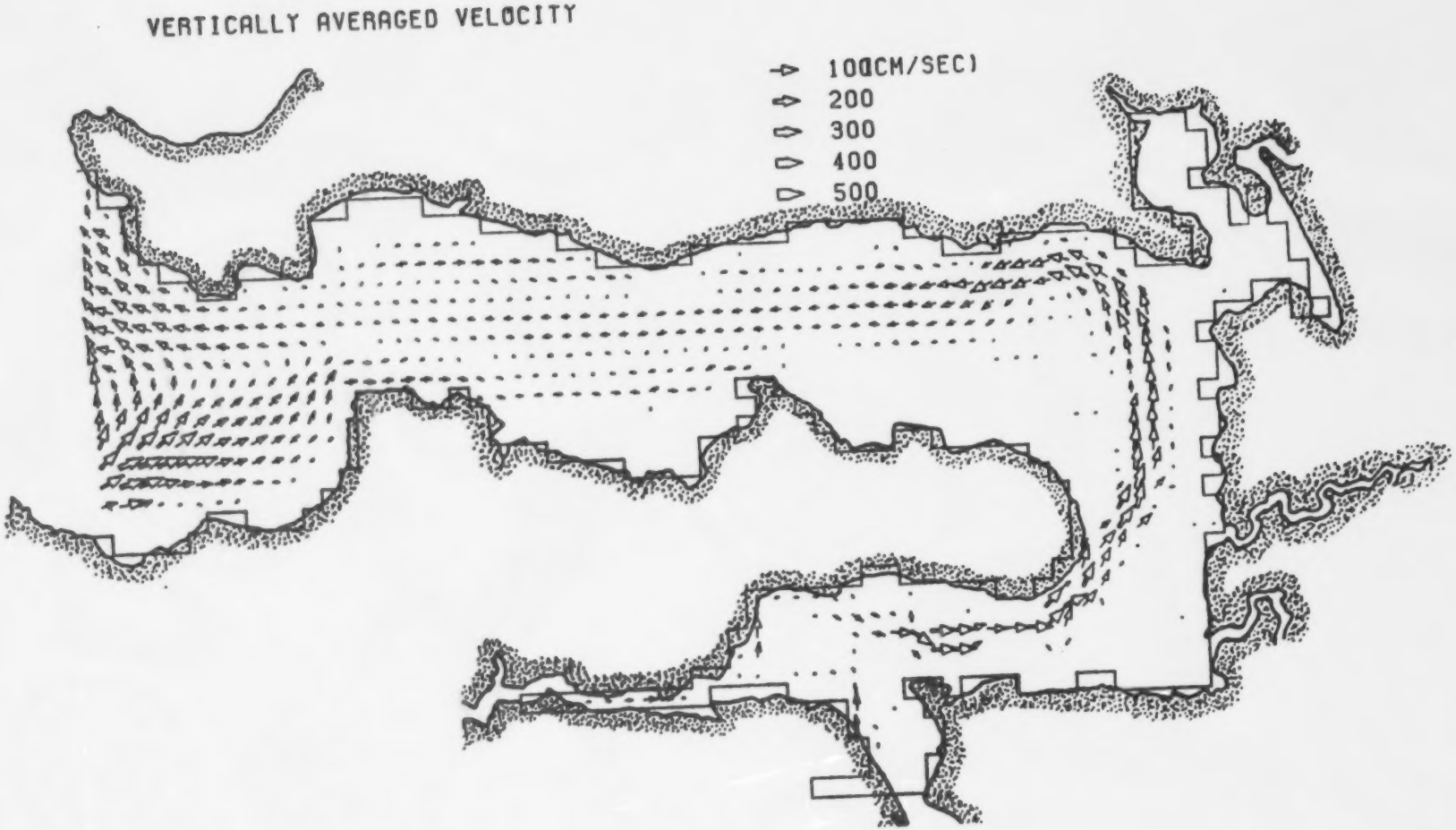

Figure 4-5 M_2 current regime at low tide, under natural conditions

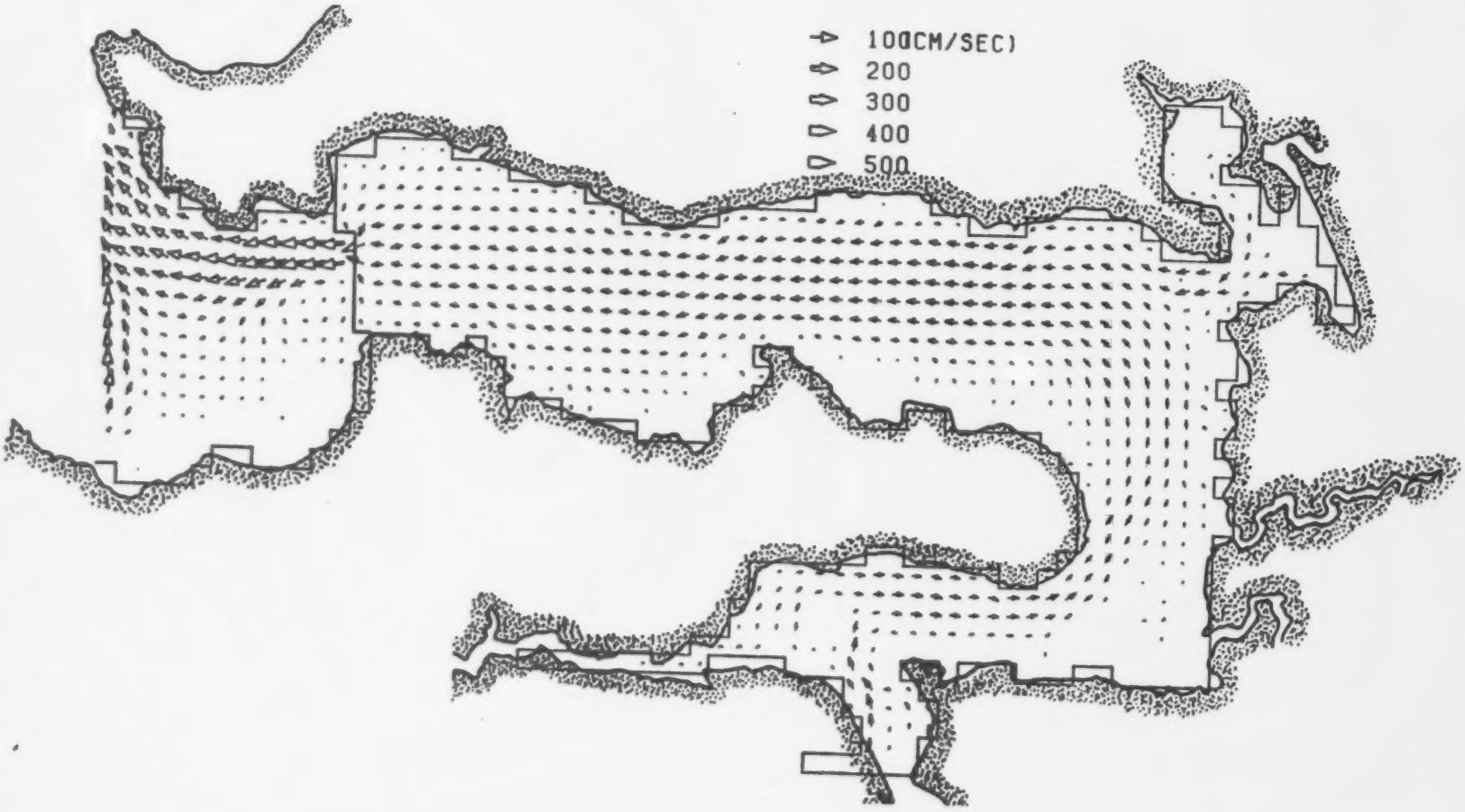

Figure 4-6 Current regime in Cumberland Basin with the A8 barrage in operation, at low tide

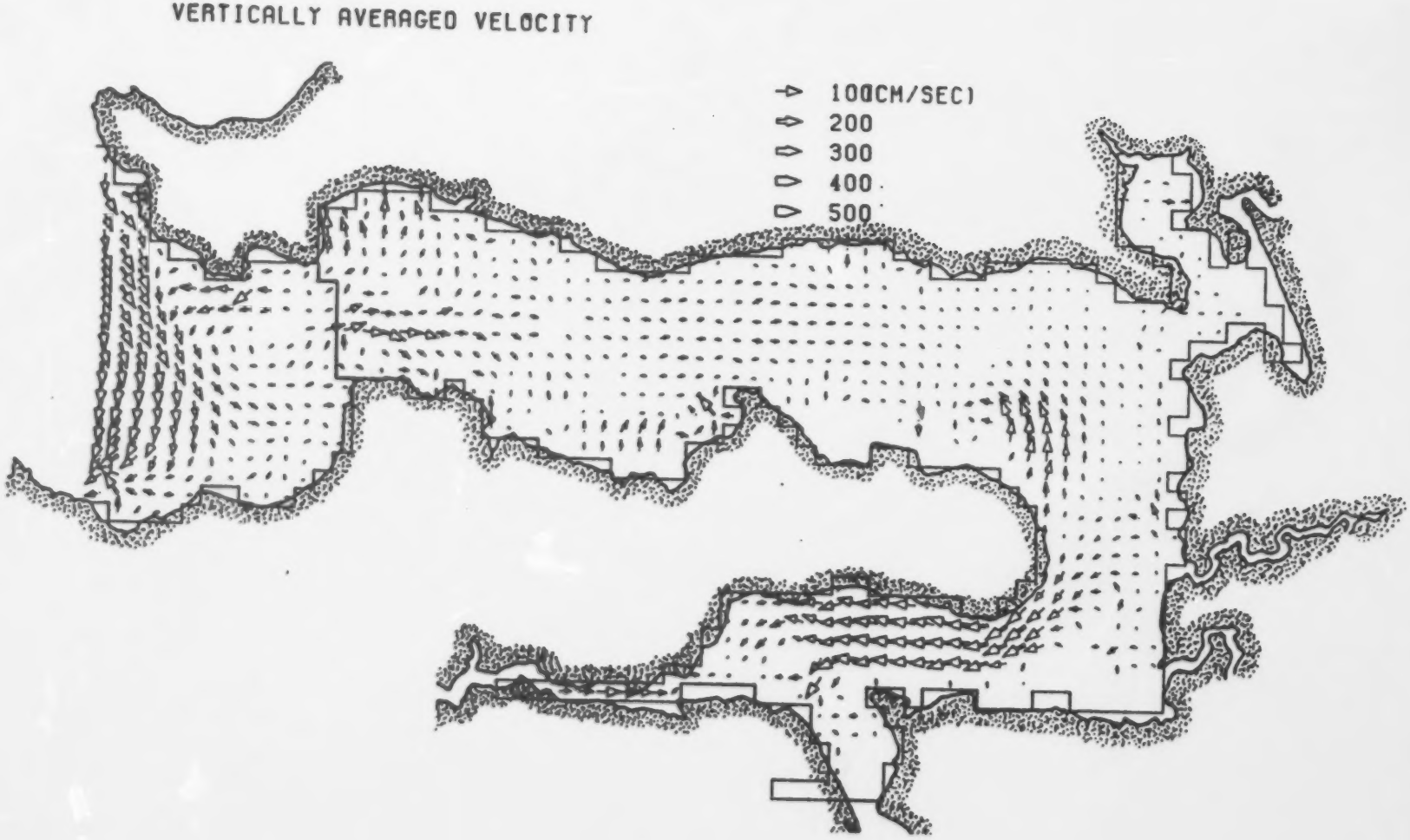

Figure 4-7 Current regime in Cumberland Basin with the A8 barrage in operation, at high tide

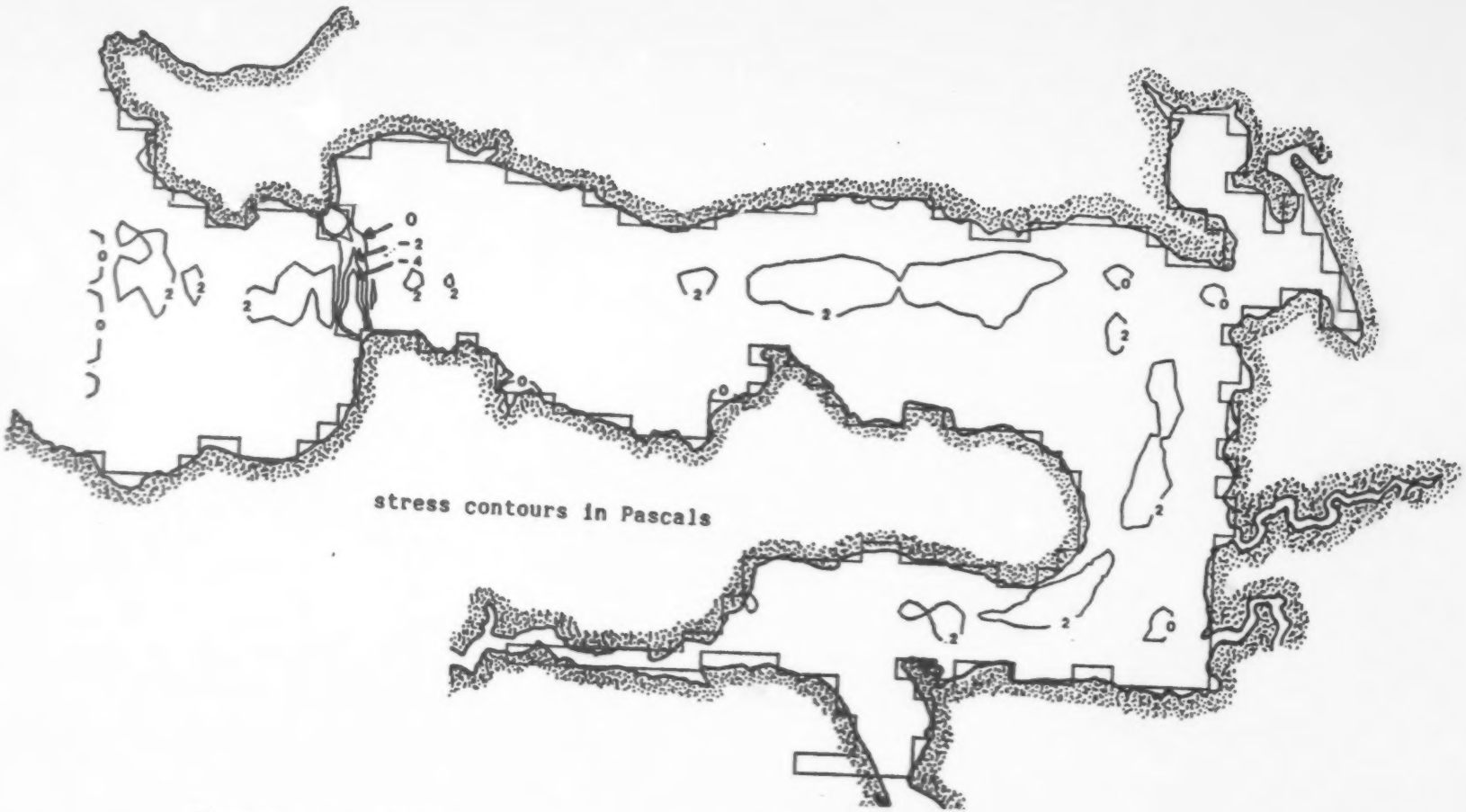

Figure 4-8 Difference in mean magnitude of bottom stress due to barrage operation

post-barrier) due to barrier operation. These features may be expected to have major impacts on the sedimentation regime of Cumberland Basin.

In the second simulation run, the placement of the sluices and turbines were drastically altered. The turbines were moved to the southern end of the barrage, and the sluices were moved to the northern end. In this configuration the turbines operate in substantially shallower water than before. It is considered that this barrage layout would be physically possible, but extremely unlikely. The tidal currents for this barrage scenario (Figure 4-9) show a large amount of variability and eddy motion compared to the results for the normal barrage. In this configuration the current velocity can approach the shallow water wave celerity in certain regions. This, combined with the effects of bottom topography, may induce flow instabilities which should be investigated further if such a barrage geometry were considered.

It is recognized that yet many unexplored possibilities remain as to the use of the model for considering other scenarios, but these are beyond the scope of the present project. There are many applications for which this model may be used. A number of them are discussed briefly below.

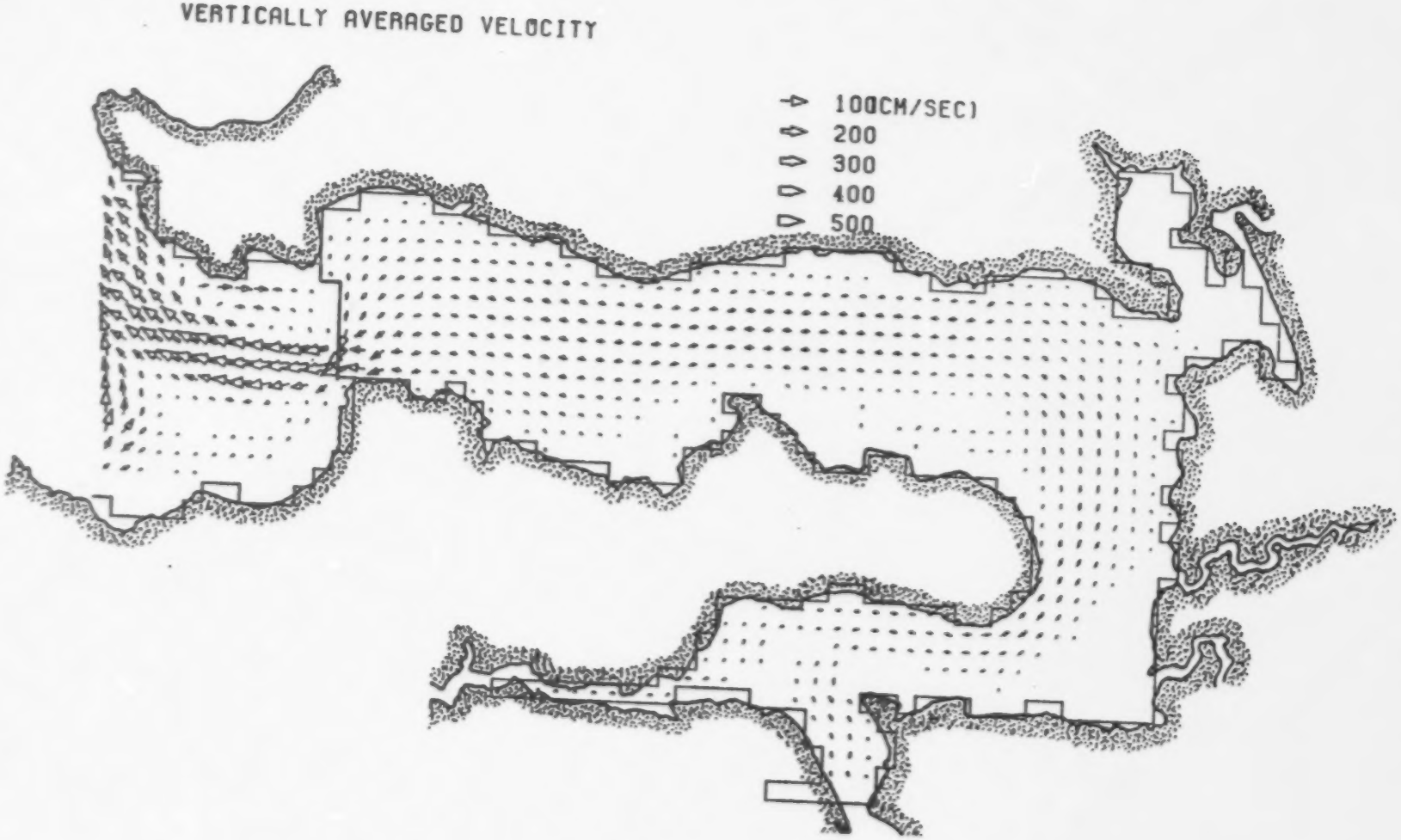

Figure 4-9 Tidal currents at low tide with a modified barrage configuration

- The effects of the alteration of the flow through the turbines and sluices on the tidal regime of Cumberland Basin may be investigated. The user of the model is presented with a high degree of flexibility in being able to to make alterations to the barrage flow; for example the volume flow through the turbines and sluices and the starting and ending heads for generation may be varied.

- An investigation may be performed to examine the effect of making changes to the placement of the sluices and turbines in the barrage. The resulting changes in the flow patterns may then be mapped.

- The output of the model may be used to make a preliminary assessment of erosion and deposition patterns both before and after the construction of a tidal power barrage.

- The model could be used to make an assessment of the variability of turbidity in the area and its effect on the biology of the region.

- It could become the tidal sub-model for the Cumberland Basin ecosystem model.

- The methodologies developed as a result of this contract can be applied to other areas.

4.6 High Current Locations for Current-driven Turbines

An additional purpose of this work is to identify and recommend possible high tidal current locations in the Cumberland Basin, for the purpose of making future assessments of the feasibility of surface-mounted or sea-floor mounted small scale tidal power applications.

The currents for the natural regime are generally about 1.5 m/s everywhere in the basin. The highest current velocities are just off Boss Point, being about 1.7 m/s. From Minudie Point inwards, in the channel, the M_2 currents are over 1.5 m/s.

The model developed here can be modified to accept a 'tidal fence' barrage, if it is desired to explore the cross-flow turbine concept in detail.

5.0 CONCLUSIONS AND RECOMMENDATIONS

A state of the art three-dimensional mathematical model has been implemented for Cumberland Basin. This model reproduces the vertical and horizontal flow characteristics of Cumberland Basin with the highest resolution presently practical with large main frame computers (the longest runs requiring up to 240 hours of CPU time on a CDC 830). This three dimensional representation has been shown to be crucial for horizontal dispersion (Holloway, 1982) and for the mean circulation (Wright and Loder, 1985) in the Upper Bay of Fundy. This model and the data base generated as part of the present study should provide the best basis for impact studies of tidal power development on the ecosystem, sediment and morphological regimes of Cumberland Basin.

As part of this study, a 28 day high quality record of water levels was collected in Cumberland Basin. This, together with a data set collected independently by Mount Allison University, was analyzed to provide the best estimates of tidal parameters available to date for Cumberland Basin. All available bathymetric soundings for the area were evaluated and corrected for changes in datum and horizontal references through time, to form a new consolidated bathymetric data set. These tidal and bathymetric data, generated in support of the modelling effort, are available in digital form and in themselves represent valuable output from the present study.

An examination of available data, as well as a theoretical analysis, has shown that tidal flows dominate the hydrodynamic regime of Cumberland Basin. Tidal flow exhibits a marked vertical structure, both in the oscillatory and mean components, which can only be fully accounted for by a three-dimensional analysis. To this end, an advanced mathematical model was constructed for Cumberland Basin. This model, used previously in studies of continental shelf hydrodynamics, was modified to account for mudflats and salt marshes which dry for part of the tidal cycle and represent about half of the area of Cumberland Basin. In this model, the vertical flow structure is represented continuously by a set of basis functions, a method producing more realistic profiles than discrete techniques and generally considered a preferred tool for 3-D modelling. This three dimensional representation reproduces explicitly the phenomena of vertical shear dispersion and topographically induced eddies which drive dispersion and transport mechanisms in Cumberland Basin.

A sensitivity analysis, as well as consideration of the basin topography, has confirmed that the most important length scales of Cumberland Basin are resolved by a grid size of 400m in the horizontal, and the use of six basis functions for the representation of the vertical profile. The model shows only moderate sensitivity to the specification of bottom drag coefficient and vertical turbulent diffusivity profile. Notably, the bottom stress computed from the model is much less sensitive

to the specification of drag coefficient than 2-D models, reflecting the equilibrium relationship between the flow structure and bottom boundary conditions. This should provide more reliable estimates of bottom stress for applications such as sediment transport.

The model has been verified for forcing by the single M_2 tidal frequency, as well as a full fortnightly tidal cycle with all major tidal constituents. Model calculations agree with observations within measurement accuracy. Simulations were also undertaken with the presence of a tidal barrage between Pecks Point and Boss Point (site A8). The main simulation, using a likely configuration for the placement of sluices and turbines, shows that, as expected, the tidal range, currents and bottom stresses in the head pond will be drastically reduced from natural conditions. A second simulation was undertaken with sluices and turbines placed at opposite ends of the barrages in shallower portions of the basin. The effects on tidal range were similar to the first configuration, but a large amount of variability and eddy motion was generated in the head pond. This may be attributed to the increased water velocities which at times approaches the shallow water wave celerity and, in combination with bottom topography, may induce flow instabilities.

The object of this study was to investigate the implication of tidal power development on the hydrodynamic behaviour of

Cumberland Basin. It must be realized, however, that changes in the hydrodynamics of the basin are important only inasmuch they affect the resources of the area, or their exploitation. One should not expect final answers from the present work, its value lying in the data, and the basic tool it provides for future investigations. These will include the study of any process depending on the hydrodynamics of the basin, in particular those which depend critically on bottom stresses and material transport either vertically or horizontally in the water column. This work may, therefore, form the basis of sediment transport models, ecosystem models and the study turbidity distribution as well as benthic or pelagic organism.

The data sets generated in this study, and available in the Acadia University computer archives, include simulated water levels and velocity coefficients (characterizing the vertical flow structure) for each model cell, at 15 minute time intervals, for a 14 day period (a tidal fortnight). The same is also available for 4 day simulations using M_2 tidal forcing alone, with and without the presence of a barrage. Although many analyses may be undertaken, depending on the application, only the most basic processing has been undertaken here. Further work on these data sets will depend on the specific application, but the following are of a general interest:

- Analysis of post barrage stratification potential using the H/U^3 method (Garrett et al, 1978).

- Computation of effective flushing times, horizontal and vertical mixing rates, etc.

- Computation of turbulent energy distribution.

- Calculation of the 3-D residual and tidal flow patterns through selected cross sections.

The model software can also be used to generate new data sets, for example, to investigate the effect of alternate barrage geometries. One should note, however, that better predictions will be obtained by accounting for changes in open boundary conditions caused by the presence of the barrage, a step not undertaken in the present work. As a first step one may simply reduce the tidal amplitude by 4% at the boundary as suggested by results of Greenberg (1979). Full account for this, however, would require linking the present model with a whole Bay of Fundy model such as that of Greenberg (1979), so that the dynamic coupling between Cumberland Basin and the rest of the system can be explicitly considered. Further hydrodynamic modelling studies should be undertaken to consider the effects of wind and waves, which may have a significant effect on the mean circulation of the basin, as well as on the bottom stress distribution.

6.0 BIBLIOGRAPHY

Abramowitz, M. and I. Stegun. 1965. Handbook of Mathematical Functions. Dover Publishing Inc. New York, N.Y.

Acres, H.G. & Company. 1946. Report on Tidal Power in the Petitcodiac and Memramcook Estuaries, Province of New Brunswick. Edmund Cloutier, Publisher to the King's most excellent Majesty, 1946. 2 vol.

Amos, C.L. and K.W.Asprey. 1979. Geophysical and sedimentary studies in the Chignecto Bay system. Bay of Fundy - A progress report. In: Current Research, Part B, Geol. Surv. Can. Pap. 79-1B: 245-252.

Amos, C.L. and K.W. Asprey. 1981. An interpretation of oceanographic and sediment data from the upper Bay of Fundy. Bedford Institute of Oceanography Rept. Series/BI-R-81-15, 143p.

Amos, C.L. and D.A. Greenberg. 1983. Suspended sediment transport and deposition modelling in the Bay of Fundy, N.S. A region of potential tidal power development. Can. J. Fish. Aquat. Sci., 40 (Suppl.1): 20-34.

ATPPB. (Atlantic Tidal Power Programming Board). 1969. Feasibility of tidal power development in the Bay of Fundy. Board Report and Committee Report Halifax, Nova Scotia.

BFTRB (Bay of Fundy Tidal Power Review Board). 1977. Reassessment of Fundy Tidal Power Review Board and Management Committee, Nov. 1977, 516 p.

Cant, G.P. 1986. Fundy tides in the Upper Reaches of the Cumberland Basin. Internal note # 20, Chignecto Research Group of Mount Allison University, Sackville, N.B. June, 1986.

Csanady, G.T. Turbulent Diffusion in the Environment. Reidel Dordrecht. 1973. 248 pp.

Conley, M.W., and G.R. Daborn. 1983. Energy Options for Atlantic Canada. Formac Publishers.

Daborn, G.R., ed. 1977. Fundy Tidal Power and the Environment. Acadia University Institute Publication No. 28.

de Margerie, S. and K. Lank. 1986. Tidal Circulation of the Scotian Shelf and Grand Banks. Report to the Department of Fisheries and Oceans, Contract # 08SC.FP901-5-X515.

DeWolfe, D.L. 1977. Tidal measurement program of the Bay of Fundy - Gulf of Maine tidal regime. Canadian Hydrographers Association, Lighthouse, 15, p.17.

DeWolfe, D.L. 1986. An update on the effects of tidal power development on the tidal regime of the Bay of Fundy and the Gulf of Maine. In: Effects of changes in sea level and tidal range on the Gulf of Maine - Bay of Fundy system. Acadia Centre for Estuarine Research Publication no. 1, pp. 35-54.

Discovery Consultants Ltd. 1985. An update on the effects of tidal power development on the tidal regime of the Bay of Fundy and the Gulf of Maine. Report prepared for Tidal Power Corporation, 39 pp..

Duff, G.F.D. 1981. A gulf and ocean model of the Bay of Fundy tides, and response to barrier construction and operation. Utilitas Math. 19: pp. 3-80.

Fischer, H.B. E.J. List, R.C.Y. Koh, J. Inberger and N.H. Brooks, 1979. Mixing in Inland and Coastal Waters. Academic Press Inc., N.Y. 483 pp.

Foreman, M.G.G. 1977. Manual for Tidal Heights Analysis and Prediction. Pacific Marine Sciences report 77-10. Institute of Ocean Sciences, Patricia Bay, Victoria, B.C.

Fundy Tidal Power Update Task Force. 1982. Fundy Tidal Power Update '82. Halifax, N.S.: Tidal Power Corporation. 41 pp.

Garrett, C. 1972. Tidal resonance in the Bay of Fundy and Gulf of Maine, Nature, 238 (Aug. 25): pp. 441-443.

Garrett, C. 1974. Normal modes of the Bay of Fundy and Gulf of Maine. Can. J. Earth Sci. 11 (4): pp. 549-556.

Garrett, C.J.R. 1977. Tidal influences on the physical oceanography of the Bay of Fundy and Gulf of Maine. In: Daborn, G.R., ed., Fundy Tidal Power and the Environment. Acadia University Institute Publication No. 28, pp. 101-115.

Garrett, C.J.R., J.R. Keeley and D.A. Greenberg. 1978. Tidal mixing versus thermal stratification in the Bay of Fundy and Gulf of Maine. Atmosphere - Ocean 16: pp. 403-423.

Garrett, C. and B. Toulany. 1979. A variable depth Green's function for shelf edge tides. Journal of Physical Oceanography Vol. 6 (9): pp. 1258-1272.

Gill, A.E. 1982. Atmosphere-Ocean Dynamics. Academic Press, New York. 662 pp.

Godin, G. 1968. The 1965 current survey of the Bay of Fundy. A new analysis of the data and an interpretation of the results. Manuscript Report No. 8. Energy, Mines and Resources, Ottawa, 97 pp.

Gordon, D.C. Jr., P.D. Keiser, G.R. Daborn, P.Schwinghamer and W.L. Silvert. 1986. Adventures in Holistic Ecosystem Modelling: The Cumberland Basin Ecosystem Model. Neth. J. Sea Res. 20:325-335.

Gordon, R. 1982. Wind Driven Circulation in Narragansett Bay. Ph.D. Dissertation, Department of Ocean Engineering, University of Rhode Island, Kingston, Rhode Island.

Greenberg, D.A. 1969. Modification of the M_2 tide due to barriers in the Bay of Fundy. Journal of the Fisheries Research Board of Canada 26(11): 2775-2783.

Greenberg, D.A. 1975. Mathematical studies of tidal behaviour in the Bay of Fundy. Ph.D. Thesis, University of Liverpool. 139; (Marine Sciences Directorate Manuscript Report Series 46. 127p.)

Greenberg, D.A. 1979. A numerical model investigation of tidal phenomena in the Bay of Fundy and Gulf of Maine. Marine Geodesy 2(2): pp. 161-187.

Greenberg, D.A. 1983. Modelling the mean barotropic circulation in the Bay of Fundy and Gulf of Maine. Journal of Physical Oceanography 13:886-904.

Heaps, N.S. 1972. On the Numerical Solution of the Three-Dimensional Equations for Tides and Storm Surge, Memoires Societe Royale des Liege, 6e Series, Tome I, 143-180.

Hildebrand, L.P. et al. 1980. Activities of the Job Corps Program: Fundy Tidal Power Development Project # 16-01-002N. Unpublished Manuscript, Bedford Institute of Oceanography.

Holloway, P.E. 1981. Longitudinal mixing in the upper reaches of the Bay of Fundy. Estuarine, Coastal and Shelf Science, 13: pp. 495-515.

Isaji, T., M. Spaulding, and C. Swanson. 1982. A Three Dimensional Hydrodynamic Model of Wind and Tidally Induced Flows on Georges Bank, In: Interpretation of the Physical

Oceanography of Georges Bank, EG & G Environmental Consultants report to the Minerals Management Service, Contract AAA851-CT1-39.

Isaji, T. and M. Spaulding. 1983. A model of Tidally Induced Residual Circulation in the Gulf of Maine and Georges Bank, submitted to Journal of Physical Oceanography.

Laevastu, Tavio, 1974. A Multilayer Hydrodynamical-Numerical Model (W. Hansen Type), Environmental Prediction Research Facility, Technical Note No. 2-74, Naval Postgraduate School.

Lambiase, J.J. 1977. Sediment dynamics in the macrotidal Avon River estuary, Nova Scotia, Ph.D. Thesis. McMaster University, Hamilton, Ont. 415 p.

Leendertse et al., 1973. A Three dimensional Model for Estuaries and Coastal Seas: Vol 1. Principals of Computation, R-1417-OWRR. The Rand Corporation.

Mitchell, A.R. and D.F. Griffiths, 1980. The Finite Difference Method in Partial Differential Equations. John Wylie & Son Ltd., N.Y.

Owen, A. 1980. A Three Dimensional Model of the Bristol Channel, Journal of Physical Oceanography, Vol. 10, p. 1290-1302.

Rao, D.B. 1968. Natural oscillations of the Bay of Fundy. J. Fish. Res. Bd. Can. 25: 1097-1114.

Tidal Power Consultants Ltd. 1984. Fundy Tidal Power - Stage 1. Report # TPCL-1-84.

Tee, K.T. 1977. Tide-induced residual current - verification of a numerical model. J. Phys. Oceanogr. 7(3): 396-402.

Tee, K.T. 1979. The structure of three-dimensional tide-generating currents. Part 1.: Oscillating Currents. J. Phys. Oceanogr. Vol. 9 pg. 930-944.

Tee, K.T. 1982. The structure of three-dimensional tide-generating currents; experimental verification of a theoretical model. Estuarine, Coastal and Shelf Science 14(1):27-48.

Wright, D.G. and J. W. Loder. 1985. A depth dependent study of the topographic rectification of tidal currents. Geophysical and Astrophysical Fluid Dynamics 31:169-220.

APPENDIX A Model Set-Up

Program CUMBEP reads six input files; four formatted (NR1,NR2,NR4 and TURDAT), and two unformatted (NR5 and NR6). They consist of the following:

File NR1. PARAM (Input on IO unit 5) This file contains the parameters which control the overall model simulation.

File NR2. BOUNDAT (Input on IO unit 6) This file contains the specification of the tide on the open boundary.

File NR4. GLRKINT (Input on IO unit 8) This file provides input information concerning Galerkin integrals to the model. It contains matrix elements of the Galerkin integrals, which have been pre-calculated for a maximum of 6 polynomials (MB=6). It must not be altered in any way.

File TURDAT contains the data required to specify a tidal barrage in the Cumberland Basin. It is dealt with in detail in Appendix B.

File NR5. BATHY (Input on IO unit 9) This is a binary file which contains the model bathymetry. It is not possible to alter it.

File NR6. This file is read as an initial condition for the simulation if ISTART is specified as '1' in the input module of IO parameters. The file is the output of the previous run, and hence only exists after one program execution has been completed.

The contents of each of the above files will now be discussed in some detail.

File NR1 (PARAM)

Run Parameters.

This file is a collection of indices and parameters which control individual sub-models. The inputs are made modular, so each module can be placed in any order within the file NR1. This is to be read through IO unit 5.

Within the module, however, input lines are places in order and the first line, as a header, must start with the particular four characters as shown in the following examples. In succeeding lines, the first ten columns are reserved for a variable name, the next ten columns for the actual input field, and the rest are for descriptive comments. All integer inputs are read as FORMAT(10X,I10). FORMAT(10X,I10) is used for real inputs regardless of the decimal location. The distinction between integer and real follows traditional FORTRAN, where a variable name starting with the letter I,J,K,L,M and N is integer. Otherwise all are real. The alterable data in the various modules in the file is discussed below for each module.

Computational Characteristic Module:

```
COMPUTATIONAL CHARACTERISTIC-----------------------------------
  NB      =          6          : # OF POLYNOMIALS (MAXIMUM OF 6)
  NSTORM  =          0          : <0 STORM ONLY, =0 NO STORM, >1 ALL (STEP)
  PDEPTH  =         0.          : <0 FALSE, =0 AS READ, >0 CONSTANT
  DT      =   10.00000          : TIME STEP (SEC)
  TME     =         0.          : INITIAL MODEL TIME (SEC) IF ISTART=0
  TRAMP1  =         0.          : COSINE RAMP TIME FOR OPEN B.D. (SEC)
  TRAMP2  =         0.          : COSINE RAMP TIME FOR WIND STRESS (SEC)
```

Do not alter the first line.

Alterable Data.

NB is the number of Legendre polynomials. It ranges from 1 to 6, the maximum possible value.

DT is the model time step in seconds. It should not be altered.

All other variables cannot be altered.

IO Parameters Module:

```
I/O PARAMETER----------------------------------------------------------
  MAXST  =      10000          : MODEL RUNS FOR MAXST*DT (SEC)
  NHDOUT =         90          : SOLUTION OUTPUT FREQ. (STEP)
  ISTART =          0          : =0 ZERO START, =1 READ PREVIOUS RUN
  ISTORE =          1          : =0 NOT STORE, =1 STORE PRESENT RUN
  NTPOUT =         90          : DIAGNOSTIC LISTING FREQUENCY (STEP)
  NR2    =          6          : IO UNIT # FOR OPEN BOUNDARY CONDITION
  NR3    =          7          : IO UNIT # FOR STORM TRACK
  NR4    =          8          : IO UNIT # FOR MATRIX ELEMENT
  NR5    =          9          : IO UNIT # BATHYMETRY
  NR6    =         10          : IO UNIT # FOR RESTART DATA
  NW1    =         11          : IO UNIT # FOR OUTPUT LISTING
  NW2    =         12          : IO UNIT # FOR SOLUTION OUTPUT
  NW3    =         13          : IO UNIT # FOR TIME SERIES OUTPUT
  NW4    =         14          : IO UNIT # FOR THE LAST SOLUTION
```

Do not alter the first line.

MAXST is the maximum time steps for the simulation to continue. The simulation always runs for MAXST steps (MAXSTxDT) seconds in time) regardless of the present time and step upon model initiation.

NHDOUT is the frequency of solution output in units of time steps. No output results if NHDOUT is zero or greater than MAXST.

ISTART If ISTART is 0, the simulation starts with the hydrodynamic variables (currents and elevations) approximating conditions at high tide. If it is '1', the previous solution is read as the initial condition.

ISTORE controls output of the last solution step. If it is '1', the solution is written to the file NW4 for a succeeding run. If it is zero, no output results.

NTPOUT is the step frequency of a diagnostic listing (on file NW1). The diagnostic listing consists of the term balance and the velocity profile for a pre-selected grid cell. The grid cell is chosen to be the first cell specified in the input module of Time Series Output. If there is no location specified (NLOC = 0), it is substituted by the middle number of the sequential grid count.

NR2,NR3,NR4 and NR5 are FORTRAN IO numbers, all to be read. Usage of each file is given in the input example itself.

NW1,NW2, NW3 and NW4 are IO unit numbers to which files are written.

Time Series Output Module:

```
TIME SER. OUTPUT-------------------------------------------------------
  NLOC    =          3          : # OF LOCATION FOR TIME SER. OUTPUT (<10)
  LOC # 1        -12       -26          : GRID (-I, -J)
  LOC # 2        -30       -26          : GRID (-I, -J)
  LOC # 3        -46       -28          : GRID (-I, -J)
```

Do not alter the first line.

The program writes the the solution values and hydrodynamic term balances for preselected cell locations.

NLOC defines how many of the above cells are requested. The maximum allowed is nine. The program then reads NLOC lines. NLOC can be less than the total number of lines succeeding. The total output of points is determined by NTPOUT. The user must provide one cell location per line. The cell location is specified with grid indices (i,j). The values must be negative. Also note the format is (10X,2I10) and is an exception. Three lines are shown in the example.

Internal Stress Module:

```
INTERNAL STRESS-------------------------------------------------
 IVEDDY  =          5          : 1=CNST 2=DEPTH 3=WIND 4=PBOL 5=SPL
 VEDY0   =  500.0E-4           : M2/SEC ( CM2/SEC * E-4)
 VEDY1   =  050.0E-4
 VEDY2   =  500.0E-4
 NZ      =          2          : # OF PTS. INCL. SURFACE AND BOTTOM
  Z,V    =        0.0 10000.E-4
  Z,V    =      100.0     0.E-4
```

The values in the internal stress module should not be altered.

Bottom Stress Module:

```
BOTTOM STRESS---------------------------------------------------
  CDF    =    +0.0030          : BOTTOM FRICTION (NON-D), CFD<0 BBL MODEL
  CKB    =        0.0          : PHYSICAL BOTTOM ROUGHNESS (CENTIMETER)
  GD     =      0.000          : BOTTOM GRAIN DIAMETER(CENTIMETER)
```

The values in the bottom stress module should not be altered.

Horizontal Stress Module:

```
HORIZONTAL STRESS-------------------------------------------------
  NSMOV  =          5          : 2-D VELOCITY SMOOTHING FREQ.(STEP)
  NSMOS  =          0          : SEA SURFACE --(0 FOR NO SMOOTHING)--
  SMOV2  =      0.990          : 2-D VELOCITY SMOOTHING WEIGHT
  SMOV3  =      0.980          : 3-D        --(1.0 FOR NO SMOOTHING)--
  SMOS   =      1.000          : SEA SURFACE
```

The values in the horizontal stress module should not be altered.

File NR2. BOUNDAT

Open Boundary Conditions.

A copy of the file BOUNDAT is shown below.

```
  NTIDE  =          1
(I5,2I4,6X,I1,F7.2,F8.3,E12.6)
  208    1   17    2   4.78    0.016 0.140519E-3
  224    1   18    2   4.78    0.013 0.140519E-3
  245    1   19    2   4.78    0.011 0.140519E-3
  271    1   20    2   4.78    0.009 0.140519E-3
  311    1   21    2   4.79    0.007 0.140519E-3
  359    1   22    2   4.79    0.005 0.140519E-3
  408    1   23    2   4.79    0.003 0.140519E-3
  461    1   24    2   4.79    0.002 0.140519E-3
  520    1   25    2   4.80    0.000 0.140519E-3
  578    1   26    2   4.80    6.281 0.140519E-3
  639    1   27    2   4.80    6.280 0.140519E-3
  701    1   28    2   4.80    6.278 0.140519E-3
  765    1   29    2   4.80    6.276 0.140519E-3
  823    1   30    2   4.81    6.276 0.140519E-3
  866    1   31    2   4.81    6.274 0.140519E-3
  892    1   32    2   4.81    6.273 0.140519E-3
  910    1   33    2   4.81    6.271 0.140519E-3
  920    1   34    2   4.82    6.269 0.140519E-3
  925    1   35    2   4.82    6.269 0.140519E-3
```

The first line in this file specifies the number of tidal constituents at the open boundary, NTIDE. A value of zero implies no tide. For this model the value is always 1.

The second line contains the format specification by which the model reads the open boundary data. It must not be altered.

The remaining lines contain the data for the open boundary in seven columns, one line for each cell on the open boundary. Columns 1 to 4 must not be altered. It is structured as follows:

Column 1. The grid sequence number of the cells along the open boundary.of the fine grid model.

Column 2. The i index of the open boundary cell.

Column 3. The j index of the open boundary cell.

Column 4. This position is occupied by a 2. It is a flag indicating to the model that only elevations are specified on the open boundary.

Column 5. The amplitude of the M_2 tide in metres at the centre of the specified cell.

Column 6. The phase of the M_2 tide in radians at the center of the specified cell.

Column 7. The frequency in radians/sec of the M_2 constituent at the centre of the specified cell.

APPENDIX B Barrage Set-Up

The configuration of the barrage is given in a data file called TURDAT. The manipulation of the values in this file allow the user to make the necessary changes to the barrage geometry, and exercise control over the characteristics of both the sluices and the turbines.

In making changes to the data file, it is important to note that the numbers in the file can be either integer or real values. A real number is followed by a period (.) and an integer is not. It is important that the TURDAT parameters preserve their integer or real characteristics.

An example of the barrage data file is given below.

```
8  4.98 1.50
1 13 29 0. 0. 0
2 13 29 0. 0. 0
1 14 28 1. 4301. 17
1 14 27 1. 4554. 18
1 14 26 0. 23703. 0
1 14 25 0. 0. 0
1 14 24 0. 0. 0
2 14 24 0. 0. 0
```

The first line of the data file has three parameters which can be modified to suit the particular run. They are:

a. The number of grid sections. It is an integer value and in the above example it is set to 8. The number of lines in the data file that follow the first line is equal to this value.

b. Starting head (in metres) for power generation. It is a real value and in the above example it is set to 4.98.

c. Ending head (in metres) for power generation. This is the value of the head at which the turbines are stopped. It is a real value and is set to 1.50 in the example.

The remaining lines in the data file contain the information necessary to completely specify the barrage. The user can manipulate these values to achieve a wide variety of barrage configurations. Each of these lines contain six numbers. A description of their significance follows.

Position 1. The value determines whether the barrage segment described by this line is on a U-line or a V-line. It has the value of 1 if it is a U-line and a value of 2 if it is a V-line.

Position 2. This is the i index of a grid line.

Position 3. This is the j index of a grid line.

Position 4. The value of this parameter indicates whether or not the barrage segment contains turbines. If it does, the value is set to 1., otherwise it is set to 0.

Position 5. This parameter specifies the flow through the barrage segment in cubic metres per second, for a one metre head. If the value is zero, then there is no flow.

Position 6. This parameter indicates the number of turbines that are included in the barrage segment. A value of zero indicates that there are no turbines.

The above datafile is set up to simulate the A8 barrage as illustrated in Update '82. The length of the barrage is eight segments (grid cells) long and crosses the Cumberland Basin at the correct location. The second and last sections are V-lines, which make the barrage have a slight 'dog-leg' at each end. Refer to Figure 4-2. The balance of the segments are U-lines. The shape of the barrage is a consequence of the fact that the flow can only be specified at the edge of a cell and therefore the barrage must follow the cell boundaries.

In the example, there are 17 turbines in the U-section at the [i,j] grid index (14,28). A '1.' in the fourth position signifies that the flow through this cell is turbine flow, with a flow of 4301 m^3/s at a 1 metre head. This value is for the 17 turbines combined. The next line indicates that 18 turbines are in the U-section at the [i,j] grid index (14,27). The flow is 4554 m^3/s. Sluice flow is specified in the [i,j] grid index (14,26). The presence of a zero in position 4 combined with a flow in position 5 indicates a sluice. The flow is for 24 sluices, each with a flow of 987.62 m^3/s, for a combined flow of 23703 m^3 /sec. The remainder of the barrage sections have no flow.

Changing the Barrier - An Example.

Suppose that it is desired to place 12 standard (12.2 m by 12.2 m) sluices in between the turbines, and move the 18 turbines to the position formerly occupied by the sluices. The turbines will start generation at a head of 4.2 metres, and shut down at 1.4 metres. The data file would now look like

```
8  4.20 1.40
1 13 29 0. 0. 0
2 13 29 0. 0. 0
1 14 28 1. 4301. 17
1 14 27 0. 11851. 0
1 14 26 1. 4554. 18
1 14 25 0. 0. 0
1 14 24 0. 0. 0
2 14 24 0. 0. 0
```

APPENDIX C. Model Output and Analysis of Results.

Output Description.

Upon the execution of program CUMBER, four output files IO unit numbers NW1, NW2, NW3, and NW4, are written. Only the first file is written formatted and is immediately legible after execution. The rest of the files are un-formatted. The content and purpose of the files are described briefly.

Output Listing (File NW1) (OUTLIST) (IO unit 11)

This file contains a listing of input parameters in Appendix A. The rest of the file contains repeated listing of term balance, stress, and velocity profile for the specified grid cell. If there is no location specified (NCLOC = 0), it is substituted by the middle number of the sequential grid cell count. The frequency of the listing is controlled by the parameter NTPOUT in the input module of IO parameters. Between the listings, there may be messages denoting a specific event or an error.

Solution Output (File NW2) (SOLUT) (IO unit 12)

The program outputs solution variables for the entire grid cells at every NHDOUT-th step. The variables include time step, model time, water elevation, coefficients describing velocity profile, and bottom friction.

Time Series Output: (NW3) (TSOUT) (IO unit 13)

The program writes temporal values of the variables for pre-selected grid cells often enough to observe the model dynamics in time. The variables written include time step, model time, sequential code number of the cell, cell flag, sea elevation, bottom friction coefficient and term balance for all terms.

Last values (File NW4) (LASTV) (IO unit 14)

This file is identical to file NW2, but written at the last time step, so that the simulation can continue by re-entering these values as initial conditions.

Analysis

The model does not compute the amplitude and phase of the M_2 tidal elevation and current during the course of a simulation. This information is obtained by performing a Fourier analysis of the the model solution output which has been written to disk on file NW2 (SOLUT). Stored in this disk file are the values of elevation and current for each grid cell of the model at an interval of NHDOUT time steps, for each of the six Legendre polynomials.

Input:

1. The values of the elevation (Z) and current (U and V components) from the model solution file SOLUT. This data file is read on unit 11.

2. A line specifying
   a) the number of parameters to be analyzed (IALIM)
   b) the number of harmonics to be analyzed (IHLIM)
   c) the time-step at which the analysis is started (START)
   d) the period in hours over which the data is to be analyzed. (PERIOD)

These values are read in free format from a data line in the job submit file.

IALIM is determined according to the following table:

IALIM	Z	U Legendre Polynomial 1	2	3	4	5	6	V Legendre Polynomial 1	2	3	4	5	6
1	x												
2	x	x											
3	x	x						x					
4	x	x	x					x					
5	x	x	x					x	x				
6	x	x	x	x				x	x				
7	x	x	x	x				x	x	x			
8	x	x	x	x	x			x	x	x			
9	x	x	x	x	x			x	x	x	x		
10	x	x	x	x	x	x		x	x	x	x		
11	x	x	x	x	x	x		x	x	x	x	x	
12	x	x	x	x	x	x	x	x	x	x	x	x	
13	x	x	x	x	x	x	x	x	x	x	x	x	x

It should be noted that the number of parameters that are analyzed for each value of IALIM are additive; for example, when IALIM equals 5, the analysis is performed on Z, plus the U and V components of the first and second order Legendre Polynomials.

IHLIM is the number of harmonics to be analyzed. For example, a value of 1 is used for an analysis of M_2; a value of 2 would yield an analysis for both M_2 and M_4.

START is the time step at which the analysis is to commence.

PERIOD is the period, in hours, for which the analysis is to be performed. A period of 12.421 hours would be used for an analysis of one tidal cycle, commencing at time step START, and continuing for 4472 time steps of 10 sec. each. Care should be taken to ensure that there is enough data after ISTART to completely fill the period of analysis. It is customary to perform the analysis on the last complete tidal cycle.

OUTPUT

The results of the Fourier analysis may be written to the line printer or to a disk file. The model grid (38 X 66 cells) is too large to be written on one page, so each parameter is output in two blocks of 19 columns by 66 rows. The first block contains the results of the array elements i=1,66 and j=1,19; (south and east half of Cumberland Basin) the second contains elements i=1,66 and j=20,38. The blocks are separated by a blank line. Non active cells can be printed as zeros or sometimes as some constant.

The parameters are output in the order mean value, amplitude and phase, according to the schedule determined by IALIM, above. The units of the mean value and amplitude are in centimetres and the units of the phase are in degrees relative to Atlantic Standard Time (AST).

The values of the various parameters specified by IALIM are printed one after the other. For example, if IALIM is specified to be 8, then the following output is produced:

1. Mean value, ζ
2. amplitude, ζ
3. phase, ζ
4. mean value, U, polynomial 1
5. amplitude, U, " 1
6. phase, U, " 1
7. mean value, V, polynomial 1
8. amplitude, V, " 1
9. phase, V, " 1
10. mean value, U, polynomial 2
11. amplitude, U, " 2
12. phase, U, " 2
13. mean value, V, polynomial 2
14. amplitude, V, " 2
15. phase, V, " 2
16. mean value, U, polynomial 3
17. amplitude, U, " 3
18. phase, U, " 3
19. mean value, V, polynomial 3
20. amplitude, V, " 3
21. phase, V, " 3
22. mean value, U, polynomial 4
23. amplitude, U, " 4
24. phase, U, " 4
26. mean value, V, polynomial 4
26. amplitude, V, " 4
27. phase, V, " 4

APPENDIX D Glossary of Oceanographic and Technical Terms

amplitude - One-half the range of a constituent tide. By analogy, it may be applied also to the maximum speed of a constituent current.

corange line - A line passing through places of equal tidal range.

cotidal line - A line on a map or chart passing through places having the same cotidal hour.

current - Generally, a horizontal movement of water. Currents may be classified as tidal and nontidal. Tidal currents are caused by gravitational interactions between the sun, moon, and earth and are a part of the same general movement of the sea that is manifested in the vertical rise and fall, called tide. Tidal currents are periodic with a net velocity of zero over the particular tidal cycle. Nontidal currents include the permanent currents in the general circulatory systems of the sea as well as temporary currents arising from more pronounced meteorological variability.

datum (vertical) - For marine applications, a base elevation used as a reference from which to reckon heights or depths. It is called a tidal datum when defined by a certain phase of the tide. Tidal datums are local datums and should not be extended into areas which have differing topographic features without substantiating measurements. In order that they may be recovered when needed, such datums are referenced to fixed points known as bench marks.

ebb tide - The movement of a tidal current away from shore or down a tidal river or estuary. In the mixed type of reversing tidal current, the terms greater ebb and lesser ebb are applied respectively to the ebb tidal currents of greater and lesser speed of each day. The terms maximum ebb and minimum ebb are applied to the maximum and minimum speeds of a current running continuously ebb, the velocity alternately increasing and decreasing without coming to a slack or reversing. The expression maximum ebb is also applicable to any ebb current at the time of greatest speed.

eddy - A quasi-circular movement of water whose area is relatively small in comparison to the current with which it is associated.

flood tide - The movement of a tidal current toward the shore or up a tidal river or estuary. In the mixed type of reversing current, the terms greater flood and lesser flood are applied respectively to the flood currents of greater and

lesser speed of each day. The terms maximum flood and minimum flood are applied to the maximum and minimum speeds of a flood current, the speed of which alternately increases and decreases without coming to a slack or reversing. The expression maximum flood is also applicable to any flood current at the time of greatest velocity.

harmonic analysis - The process by which the observed tide or tidal current at any place is separated into basic harmonic constituents.

harmonic constants - The amplitudes and epochs of the harmonic constituents of the tide or tidal current at any place.

K_1 - Lunisolar diurnal constituent. This constituent, with O_1, expresses the effect of the moon's declination. They account for diurnal inequality and, at extremes, diurnal tides.

K_2 - Lunisolar semi-diurnal constituent. This constituent modulates the amplitude and frequency of M_2 and S_2 for the declinational effect of the moon and sun respectively

L_2 - Smaller lunar elliptic constituent. This constituent, with N_2, modulates the amplitude and frequency of M_2 for the effect of variation in the moon's orbital speed due to its elliptical orbit.

M_2 - Principal lunar semidiurnal constituent. This constituent represents the rotation of the earth with respect to the moon.

N_2 - Larger lunar elliptic constituent. See L_2

O_1 - Lunar diurnal constituent. It has a period of 1.076 days. See K_1.

S_2 - Principal solar semidiurnal constituent. This constituent represents the rotation of the earth with respect to the sun.

semidiurnal - Having a period or cycle of approximately one-half of a tidal day. The predominating type of tide throughout the world is semidiurnal, with two high waters and two low waters each tidal day. The tidal current is said to be semidiurnal when there are two flood and two ebb periods each day. A semidiurnal constituent has two maxima

and two minima each constituent day, and its symbol is usually distinguished by the subscript 2.

shallow water wave - A wave is classified as a shallow water wave whenever the ratio of the depth (the vertical distance of the still water level from the bottom) to the wave length (the horizontal distance between crests) is less than 0.04.

slack water - The state of a tidal current when its speed is near zero, especially the moment when a reversing current changes direction and its speed is zero. The term is also applied to the entire period of low speed near the time of turning of the current when it is too weak to be of any practical importance in navigation. The relation of the time of slack water to the tidal phases varies in different localities. For standing tidal waves, slack water occurs near the times of high and low water, while for progressive tidal waves, slack water occurs midway between high and low water.

tidal constants - Tidal relations that remain practically constant for any particular locality. Tidal constants are classified as harmonic and nonharmonic. The harmonic constants consist of the amplitudes and epochs of the harmonic constituents, and the nonharmonic constants include the ranges and intervals derived directly from the high and low water observations.

tide - The periodic rise and fall of the water resulting from gravitational interactions between the sun, moon, and earth. The vertical component of the particulate motion of a tidal wave. Although the accompanying horizontal movement of the water is part of the same phenomenon, it is preferable to designate this motion as tidal current.

APPENDIX E Photographs

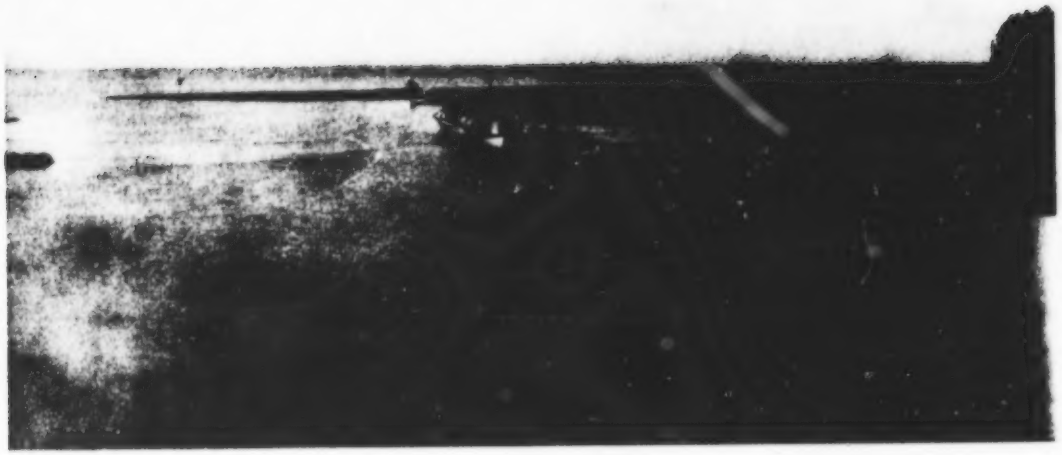

View of Allens Creek, Cumberland Basin, looking south, at high tide and low tide. The vessel in the foreground was chartered for the field program.

A view of the tide gauge mooring package, after recovery. The pressure recorder is mounted in the platform, and the pingers are secured to two of the lifting rails. There was no evidence of corrosion on the package.